

---

Multi-approach Gravity Field Models from Swarm GPS data

# Signal and error in the Swarm models up to March 2019

**Delft University of Technology (TU Delft)**  
**Astronomical Institute of the University of Bern (AIUB)**  
**Astronomical Institute Ondřejov (ASU)**  
**Institute of Geodesy Graz (IfG)**  
**Ohio State University (OSU)**

**Version 1.0**  
**2019-06-04**

Prepared and checked by  
João Encarnação  
Work Package Manager

Approved by  
Pieter Visser  
Project Manager

## Contents

<b>1 Version history</b>	<b>6</b>
<b>2 Introduction</b>	<b>7</b>
<b>3 Source data</b>	<b>7</b>
<b>4 Methodology</b>	<b>8</b>
4.1 Combination .....	8
4.2 Validation .....	8
<b>5 Results</b>	<b>11</b>
5.1 Spatial analysis .....	11
5.2 Temporal analysis .....	14
5.3 Time series of storage catchments .....	17
5.4 Temporal variability .....	35
<b>References</b>	<b>37</b>

## List of Figures

1	Time series of Satellite Laser Ranging (SLR)-derived $C_{20}$ from Cheng and Ries (2018) (blue), time series resulting from the polynomial and periodic coefficients listed in Table 3 and their difference (yellow). . . . .	9
2	Deep ocean mask. . . . .	9
3	Temporal variability of the Gravity Recovery And Climate Experiment (GRACE) prediction, including the boundaries of the regions analysed in Section 5.3.1 to Section 5.3.18. . . . .	10
4	Per-degree mean of the Root Mean Squared (RMS) difference (top) and cumulative degree-mean temporal RMS difference (bottom) between the Swarm Gravity Field Models (GFMs) and GRACE-based prediction, considering 750km Gaussian smoothing. This is (an estimate of) the average per-degree quality of the various Swarm solutions in the spectral domain (top) and globally (bottom) . The degree amplitudes remain relatively constant with increasing degree, instead of growing in terms of Equivalent Water Height (EWH), as the result of the smoothing. . . . .	11
5	Epoch-wise cumulative spatial RMS (top) and its global average (bottom) of the difference between Swarm GFMs and GRACE-based prediction, over land areas, considering 750km Gaussian smoothing. This is (an estimate of) the evolution of the ability of the various Swarm solutions to predict land mass transport processes over time (top) and its global sum (bottom). . . . .	12
6	Epoch-wise cumulative spatial RMS (top) and its global sum (bottom) of the difference between Swarm GFMs and GRACE-based prediction, over ocean areas, considering 750km Gaussian smoothing. This is the epoch-wise quality of the Swarm GFMs, and reported in the header of the combined GFMs files. . . . .	13
7	Per-degree mean (top) and its overall cumulative (bottom) of the correlation coefficient between Swarm GFMs and GRACE-based prediction, over land areas, considering 750km Gaussian smoothing. The temporal correlation at every Stokes coefficient is computed and the average over each degree is plotted at the top. It illustrates how well the temporal variations of the Swarm models agree with what is predicted from the GRACE model. . . . .	14
8	Per-degree mean (top) and its overall cumulative (bottom) of the correlation coefficient between Swarm GFMs and GRACE-based prediction, over ocean areas, considering 750km Gaussian smoothing. It illustrates that the Swarm models agree poorly with the mass variations over the ocean as predicted by the GRACE model. . . . .	15
9	Per-coefficient RMS difference between Swarm GFMs and GRACE-based prediction considering 750km Gaussian smoothing, over land (left column) and ocean (right column) areas, for AIUB, ASU, IfG, OSU and combined solutions (respectively from top to bottom). . . . .	16
10	Time series of EWH for the Amazon basin (latitude -17 to 3 degrees, longitude -76 to -47 degrees). . . . .	17
11	Time series of EWH for the Orinoco basin (latitude -3 to 12 degrees, longitude -72 to -59 degrees). . . . .	18
12	Time series of EWH for the La Plata basin (latitude -34 to -19 degrees, longitude -65 to -50 degrees). . . . .	19
13	Time series of EWH for the Mississippi basin (latitude 29 to 44 degrees, longitude -101 to -80 degrees). . . . .	20

14	Time series of EWH for the Columbia region (latitude 38 to 50 degrees, longitude -125 to -110 degrees).....	21
15	Time series of EWH for the Alaska (latitude 56 to 65 degrees, longitude -151 to -129 degrees) .....	22
16	Time series of EWH for the Western Greenland region (latitude 60 to 85 degrees, longitude -60 to -37 degrees). ....	23
17	Time series of EWH for the Danube basin (latitude 43 to 48 degrees, longitude 13 to 28 degrees). .....	24
18	Time series of EWH for the Western Sub-Saharan basin (latitude 5 to 15 degrees, longitude -15 to -1 degrees) .....	25
19	Time series of EWH for the Eastern Sub-Saharan basin (latitude 1 to 13 degrees, longitude -8 to 35 degrees) .....	26
20	Time series of EWH for the Congo and Zambezi basins (latitude -23 to -3 degrees, longitude 14 to 38 degrees).....	27
21	Time series of EWH for the Volga basin (latitude 53 to 61 degrees, longitude 34 to 56 degrees) .....	28
22	Time series of EWH for the Siberia region (latitude 57 to 72 degrees, longitude 68 to 109 degrees) .....	29
23	Time series of EWH for the Ganges-Brahmaputra basin (latitude 15 to 30 degrees, longitude 72 to 89 degrees).....	30
24	Time series of EWH for the Indochina region (latitude 12 to 29 degrees, longitude 93 to 105 degrees) .....	31
25	Time series of EWH for the Northern Australia region (latitude -24 to -10 degrees, longitude 124 to 145 degrees).....	32
26	Time series of EWH for the Western Antarctica region (latitude -80 to -70 degrees, longitude -140 to -85 degrees).....	33
27	Time series of EWH for the Eastern Antarctica region (latitude -80 to -68 degrees, longitude 80 to 130 degrees).....	34
28	Temporal variability of the individual solutions .....	35
29	Temporal variability of the combined solutions .....	36

## List of Tables

1	Overview of the gravity field estimation approaches . . . . .	7
2	Versions of the GFM <sub>s</sub> , and the Kinematic Orbit <sub>s</sub> (KOs) used in their estimation, relevant to this report. . . . .	7
3	Coefficients of the model representing the $C_{20}$ variations from Cheng and Ries (2018). . . . .	8
4	Statistics of the agreement between the GRACE and Swarm time series for the Amazon basin. . . . .	17
5	Statistics of the agreement between the GRACE and Swarm time series for the Orinoco basin. . . . .	18
6	Statistics of the agreement between the GRACE and Swarm time series for the La Plata basin. . . . .	19
7	Statistics of the agreement between the GRACE and Swarm time series for the Mississippi basin. . . . .	20
8	Statistics of the agreement between the GRACE and Swarm time series for the Columbia region. . . . .	21
9	Statistics of the agreement between the GRACE and Swarm time series for the Alaska. . . . .	22
10	Statistics of the agreement between the GRACE and Swarm time series for the Western Greenland region. . . . .	23
11	Statistics of the agreement between the GRACE and Swarm time series for the Danube basin. . . . .	24
12	Statistics of the agreement between the GRACE and Swarm time series for the Western Sub-Saharan basin. . . . .	25
13	Statistics of the agreement between the GRACE and Swarm time series for the Eastern Sub-Saharan basin. . . . .	26
14	Statistics of the agreement between the GRACE and Swarm time series for the Congo and Zambezi basins. . . . .	27
15	Statistics of the agreement between the GRACE and Swarm time series for the Volga basin. . . . .	28
16	Statistics of the agreement between the GRACE and Swarm time series for the Siberia region. . . . .	29
17	Statistics of the agreement between the GRACE and Swarm time series for the Ganges-Brahmaputra basin. . . . .	30
18	Statistics of the agreement between the GRACE and Swarm time series for the Indochina region. . . . .	31
19	Statistics of the agreement between the GRACE and Swarm time series for the Northern Australia region. . . . .	32
20	Statistics of the agreement between the GRACE and Swarm time series for the Western Antarctica region. . . . .	33
21	Statistics of the agreement between the GRACE and Swarm time series for the Eastern Antarctica region. . . . .	34
22	Statistics of the agreement between the GRACE and Swarm time series for the regions displayed in Sections Section 5.3.1 to Section 5.3.18. . . . .	35

## 1 Version history

### Version 1, 2019-06-03

- Validation of combined models version 09, from start of mission until March 2019.

## 2 Introduction

We report some statistics of the individual and combined GFMs produced on the context of the *Multi-approach Gravity Field Models from Swarm GPS data* project. The approach for combining individual gravity field solutions, i.e. those produced by the various partners mentioned in Section 3, is described in Section 4.1. The procedure and assumption used to derive the statistics is described in Section 4.2. Finally, the results are presented in Section 5.

This report does not intend to draw conclusions regarding the presented statistics, it is merely a descriptive document of the signal and error in the individual and combined Swarm GFMs. For this reason, the text in Section 5 is restricted to clarifying the quantities shown in the plots.

## 3 Source data

The individual gravity field solutions are produced by the institutes listed in Table 1.

Inst.	Approach	Reference
AIUB	Celestial Mechanics Approach (CMA) (Beutler et al. 2010)	Jäggi et al. (2016)
ASU	Decorrelated Acceleration Approach (DAA) (Bezděk et al. 2014; Bezděk et al. 2016)	Bezděk et al. (2016)
IfG	Short-Arcs Approach (SAA) (Mayer-Gürr 2006)	Zehentner and Mayer-Gürr (2016)
OSU	Improved Energy Balance Approach (IEBA) (Shang et al. 2015)	Guo et al. (2015)

**Table 1** – Overview of the gravity field estimation approaches

Additional details about the different gravity field approaches can be found in (Teixeira Encarnação and Visser, 2017).

The version of the individual GFMs is listed in Table 2.

Gravity Field Model	version	Kinematic Orbit
AIUB	01	AIUB
ASU	02	IfG
IfG	03 – 06	IfG
OSU	02	AIUB
combined	09	N/A

**Table 2** – Versions of the GFMs, and the KOs used in their estimation, relevant to this report.

The version numbers listed in Table 2 are relevant within the project and are reported so that it is possible to trace back the results presented in Section 5. Particular to the combined models, version 09 relates to the chosen combination strategy, as concluded from de Teixeira da Encarnação and Visser (2019).

## 4 Methodology

### 4.1 Combination

The combination of the models is conducted at the level of the solutions considering weights derived from Variance Component Estimation (VCE). As demonstrated in de Teixeira da Encarnação and Visser (2019), the combination at the level of Normal Equation (NEQ) disagreed more with GRACE, as a result of the vastly different amplitudes of formal errors.

The combination considers the complete degree range (degrees 2 to 40) but the VCE weights are derived from degrees 2-20. This approach addresses the very high errors above degree 20, which would otherwise drive the value of the weights.

It is feasible to determine the VCE weights because there are two time-series based on AIUB orbits (i.e. AIUB and OSU) and two time-series based on IfG orbits (i.e. IfG and ASU). Therefore the impact of the KOs on the solutions and on the VCE weights is balanced.

### 4.2 Validation

The validation is done by comparing the individual and combined solutions to a model estimated from the Release 6 (RL06) GRACE GFMs produced at Center for Space Research (CSR). This model fits a degree 1 polynomial and a yearly, semi-yearly, S2, K1 and K2 periods to the complete GRACE time series.

The  $C_{2,0}$  coefficient in all solutions has been replaced by a model fitted to the values reported in Cheng and Ries (2018). This model consists of a degree 1 polynomial and the 17 periods listed in Table 3. These periods were found empirically to minimize the residual of the model fit, which is depicted in Figure 1.

Polynomial	value	
	bias	-4.8417e-04
trend (/year)	3.9940e-12	
Periodic (years)	Sine	Cosine
1.000	6.522e-11	3.283e-11
0.500	-2.577e-11	-1.437e-11
21.728	7.605e-11	3.532e-11
2.716	-4.216e-12	-1.335e-11
1.552	-7.684e-12	-3.903e-12
5.432	-5.634e-12	2.105e-12
0.245	-9.147e-12	-1.146e-11
2.414	2.770e-12	-1.108e-11
1.975	6.942e-12	2.743e-12
0.587	4.302e-12	5.783e-12
4.346	6.809e-12	2.434e-12
1.449	7.519e-12	7.825e-13
1.035	9.589e-12	-4.015e-13
0.334	1.003e-12	8.083e-12
1.811	6.818e-12	1.809e-12
0.749	7.044e-13	-2.591e-12
0.905	1.387e-12	-9.462e-13

**Table 3** – Coefficients of the model representing the  $C_{20}$  variations from Cheng and Ries (2018).

All solutions undergo a 750km radius spherical cap Gaussian filtering, unless otherwise noted, to clearly show the geophysical signal contained in the Swarm solutions. The GRACE

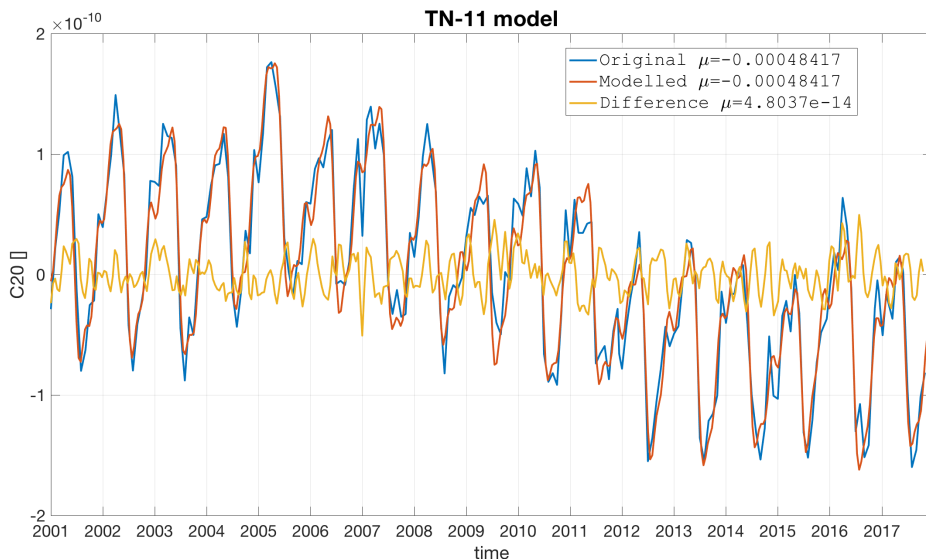


**Figure 1** – Time series of SLR-derived  $C_{20}$  from Cheng and Ries (2018) (blue), time series resulting from the polynomial and periodic coefficients listed in Table 3 and their difference (yellow).

Gravity Model 05 (GGM05G) (Tapley et al. 2013) static GFM is subtracted from all models in order to isolate the time-variable component of Earth's gravity field. We chose to show the gravity field in terms of EWH, except for the statistics related to the correlation coefficient, which are non-dimensional as usual. Both GRACE and Swarm gravity field time series are linearly interpolated to a common time domain defined by the middle epoch of the GRACE solutions and the mid-month epoch of the Swarm solutions. The analysis spans the complete Swarm mission period until March 2019.

Some analyses are restricted to either the land or ocean areas. In those cases, the land or ocean mask is applied in the spatial domain and a Spherical Harmonic (SH) analysis is done on the masked grid. The ocean mask excludes the coastal ocean areas that are roughly 1000km or less from land areas, as shown in Figure 2, while the land mask has no buffer zone.

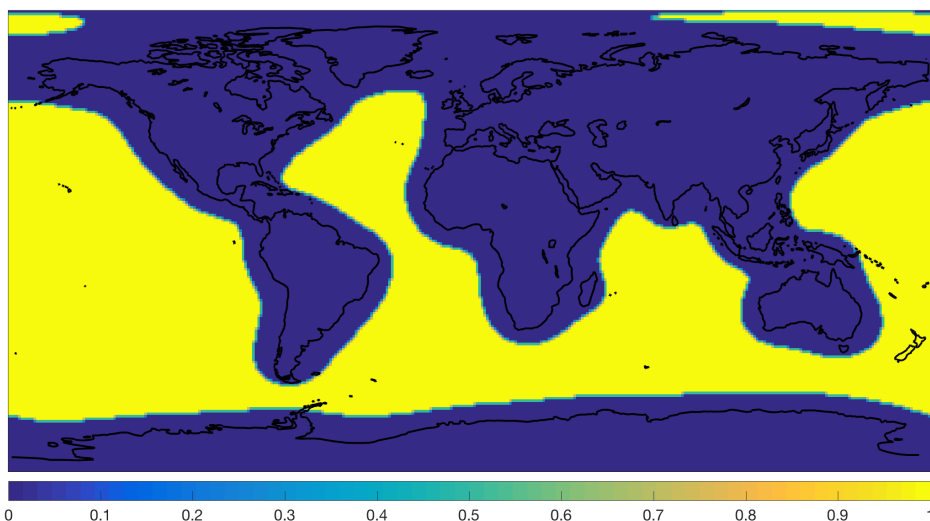


**Figure 2** – Deep ocean mask.

In Section 5.3, the geophysical signal represented by the Swarm solutions is evaluated on the basis of the time series of average EWH over restricted geographical locations, shown in Figure 3.

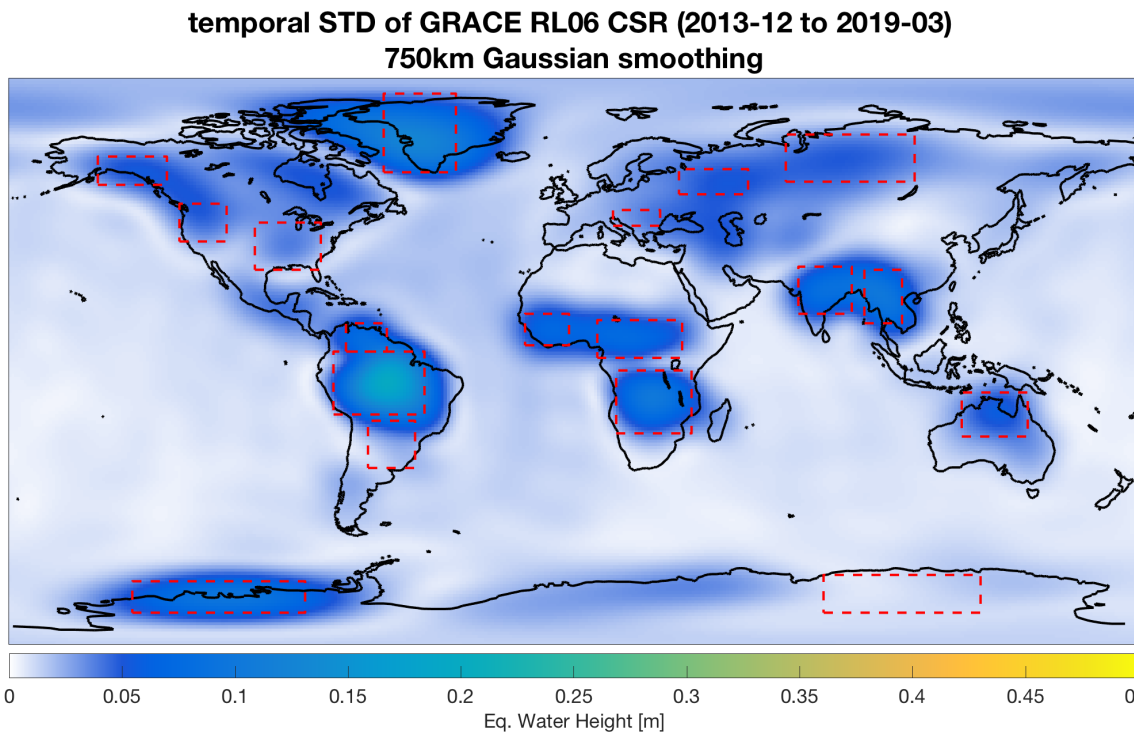


**Figure 3** – Temporal variability of the GRACE prediction, including the boundaries of the regions analysed in Section 5.3.1 to Section 5.3.18.

Each averaging is done over the corresponding spatial truncation of an equiangular grid representation of the SH coefficients. The locations shown in Sections 5.3.1 to 5.3.18 are related to the largest hydrological basins and polar regions with the highest signal variability observed by GRACE. Note that there is no effort to meticulously consider or implement proper leakage reduction methods, e.g. by Guo, Duan and Shum (2010). We perform a parametric regression on all time series considering a constant and drift terms, along with annual and semi-annual sine and co-sine terms to improve the robustness. We plot the linear part of this regression, in order to quantify the accuracy of Swarm-derived climatological trends. The time series are plotted along with tables presenting some statistics. The values of the constant and linear terms for the Swarm and GRACE solutions (column 1) are show in terms of EWH (columns 2 and 4). Additionally, the difference of these parameters between the various Swarm solutions and GRACE is listed in columns 3 and 5 (the values for GRACE in these columns is zero). Finally, the correlation coefficients between the Swarm solutions and GRACE is presented in the last column (the value for GRACE is 1). The constant term is the average basin storage at 2014-07-01.

## 5 Results

### 5.1 Spatial analysis

#### 5.1.1 Degree-mean RMS difference

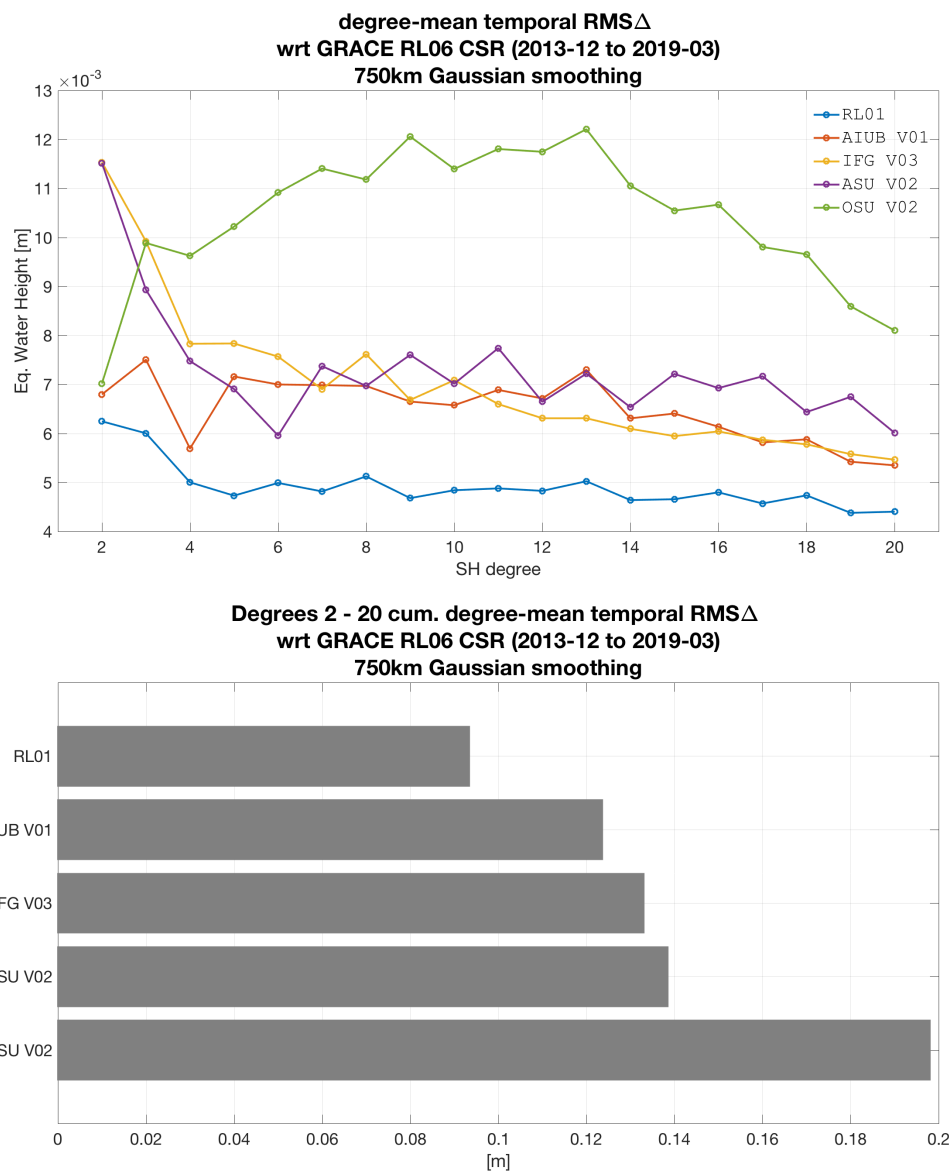


**Figure 4** – Per-degree mean of the RMS difference (top) and cumulative degree-mean temporal RMS difference (bottom) between the Swarm GFMs and GRACE-based prediction, considering 750km Gaussian smoothing. This is (an estimate of) the average per-degree quality of the various Swarm solutions in the spectral domain (top) and globally (bottom). The degree amplitudes remain relatively constant with increasing degree, instead of growing in terms of EWH, as the result of the smoothing.

### 5.1.2 Cumulative RMS difference over land

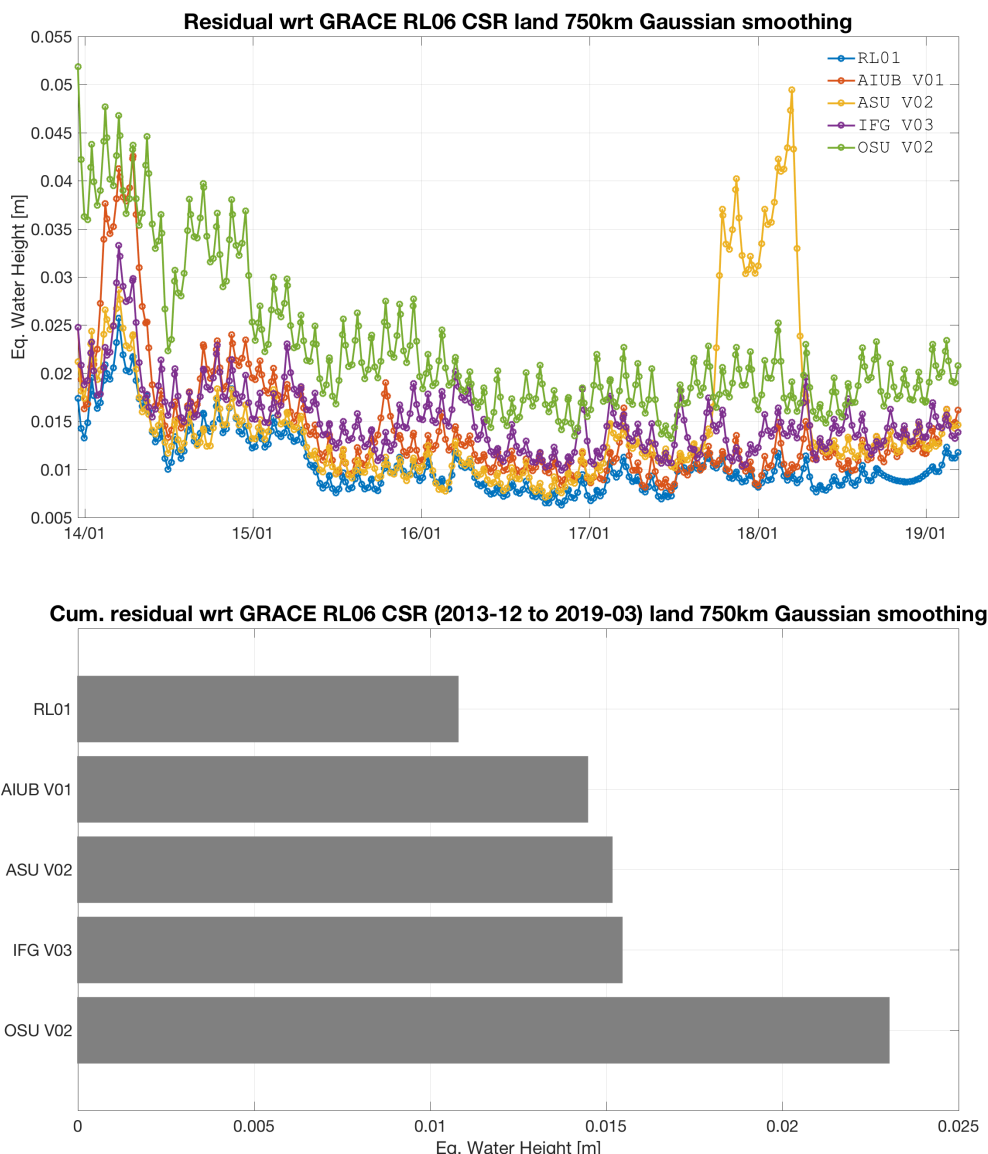


**Figure 5** – Epoch-wise cumulative spatial RMS (top) and its global average (bottom) of the difference between Swarm GFMs and GRACE-based prediction, over land areas, considering 750km Gaussian smoothing. This is (an estimate of) the evolution of the ability of the various Swarm solutions to predict land mass transport processes over time (top) and its global sum (bottom).

### 5.1.3 Cumulative RMS difference over oceans

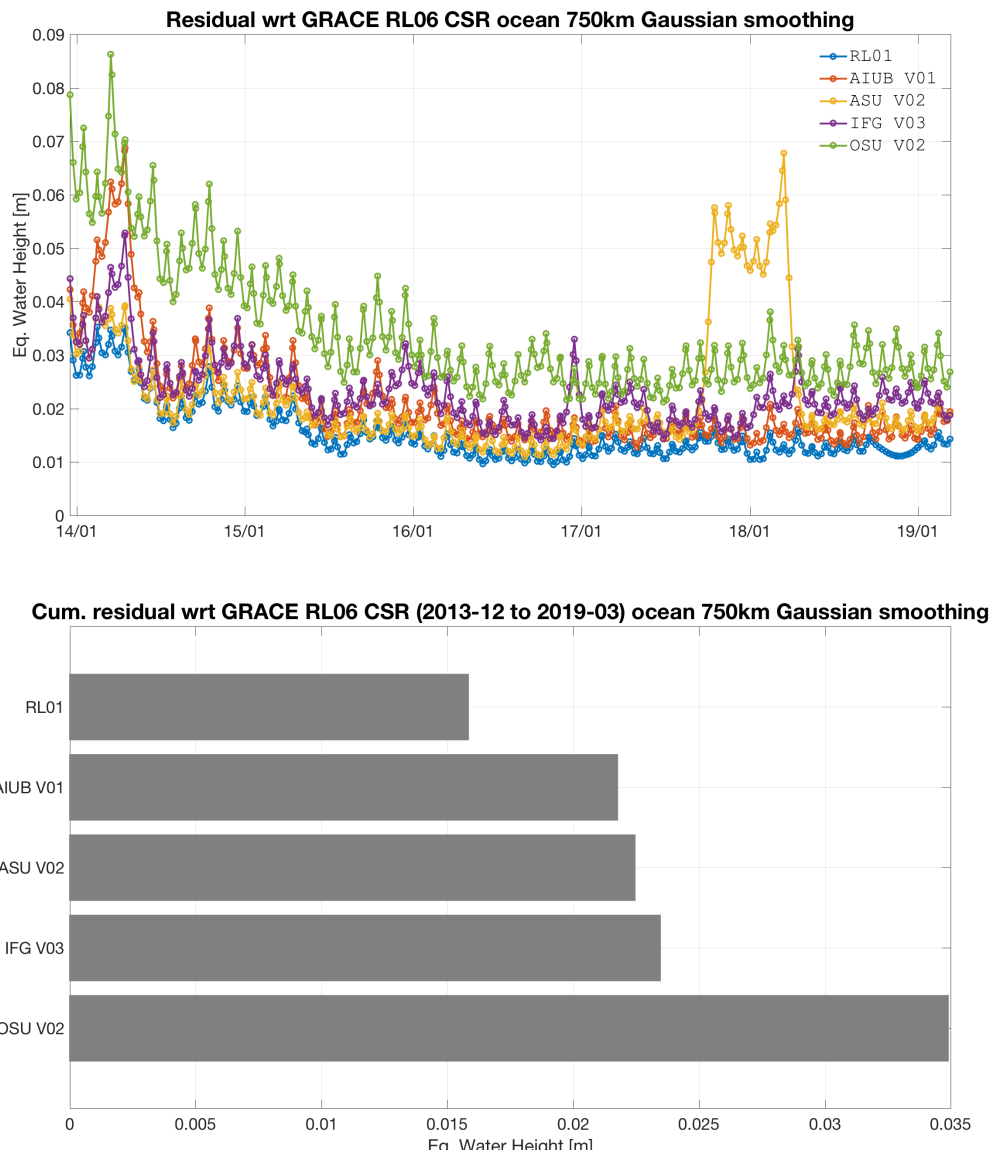


**Figure 6** – Epoch-wise cumulative spatial RMS (top) and its global sum (bottom) of the difference between Swarm GFMs and GRACE-based prediction, over ocean areas, considering 750km Gaussian smoothing. This is the epoch-wise quality of the Swarm GFMs, and reported in the header of the combined GFMs files.

## 5.2 Temporal analysis

### 5.2.1 Cumulative RMS difference over land

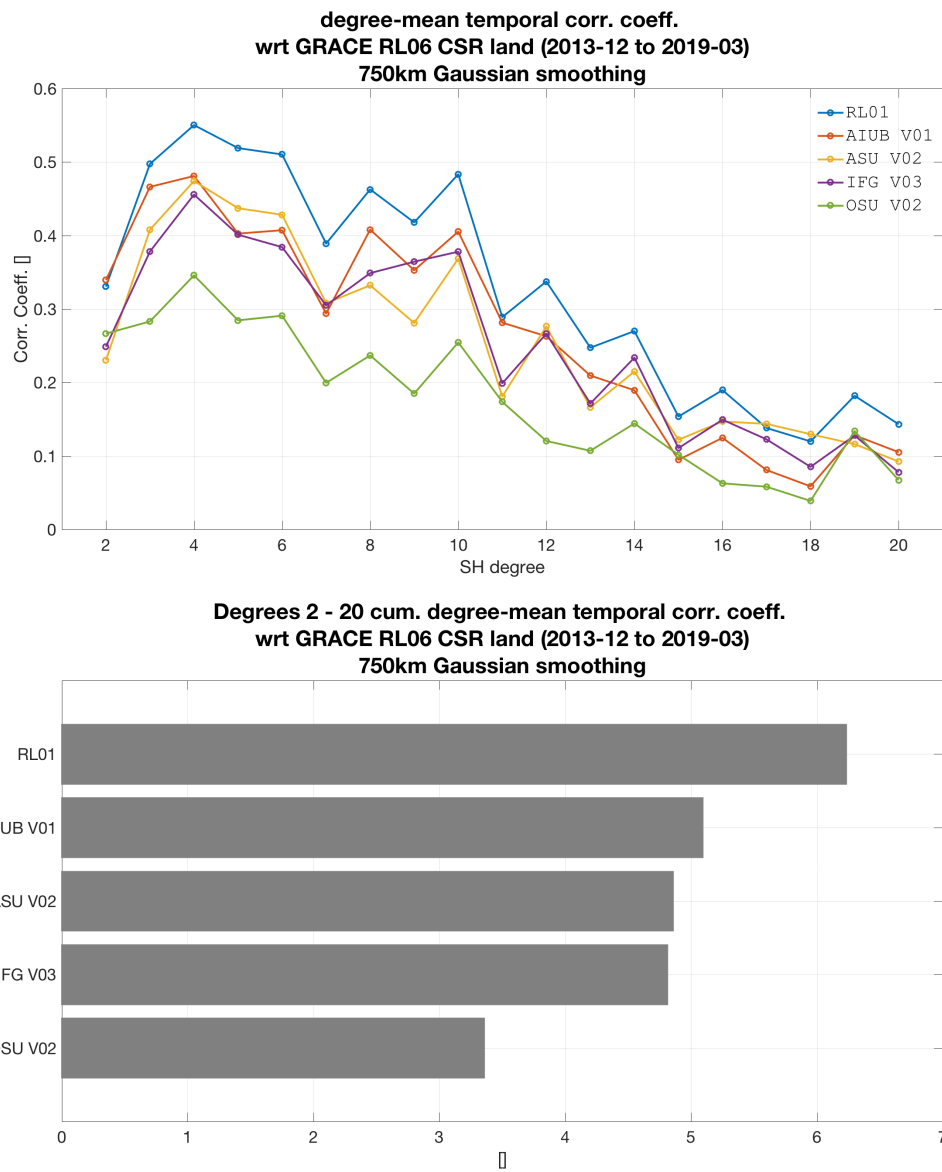


**Figure 7 –** Per-degree mean (top) and its overall cumulative (bottom) of the correlation coefficient between Swarm GFMs and GRACE-based prediction, over land areas, considering 750km Gaussian smoothing. The temporal correlation at every Stokes coefficient is computed and the average over each degree is plotted at the top. It illustrates how well the temporal variations of the Swarm models agree with what is predicted from the GRACE model.

### 5.2.2 Cumulative RMS difference over oceans

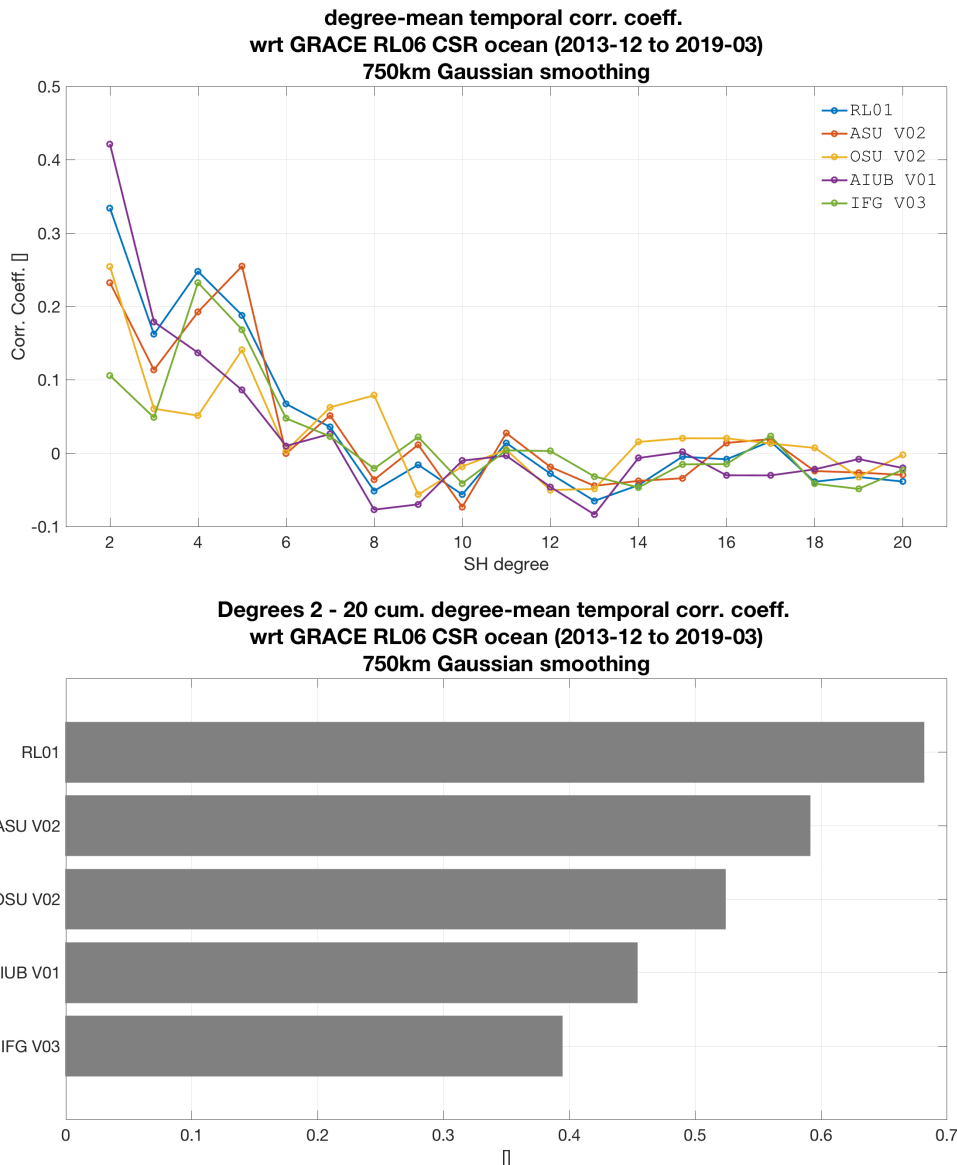


**Figure 8** – Per-degree mean (top) and its overall cumulative (bottom) of the correlation coefficient between Swarm GFMs and GRACE-based prediction, over ocean areas, considering 750km Gaussian smoothing. It illustrates that the Swarm models agree poorly with the mass variations over the ocean as predicted by the GRACE model.

### 5.2.3 Triangular plots of the RMS differences

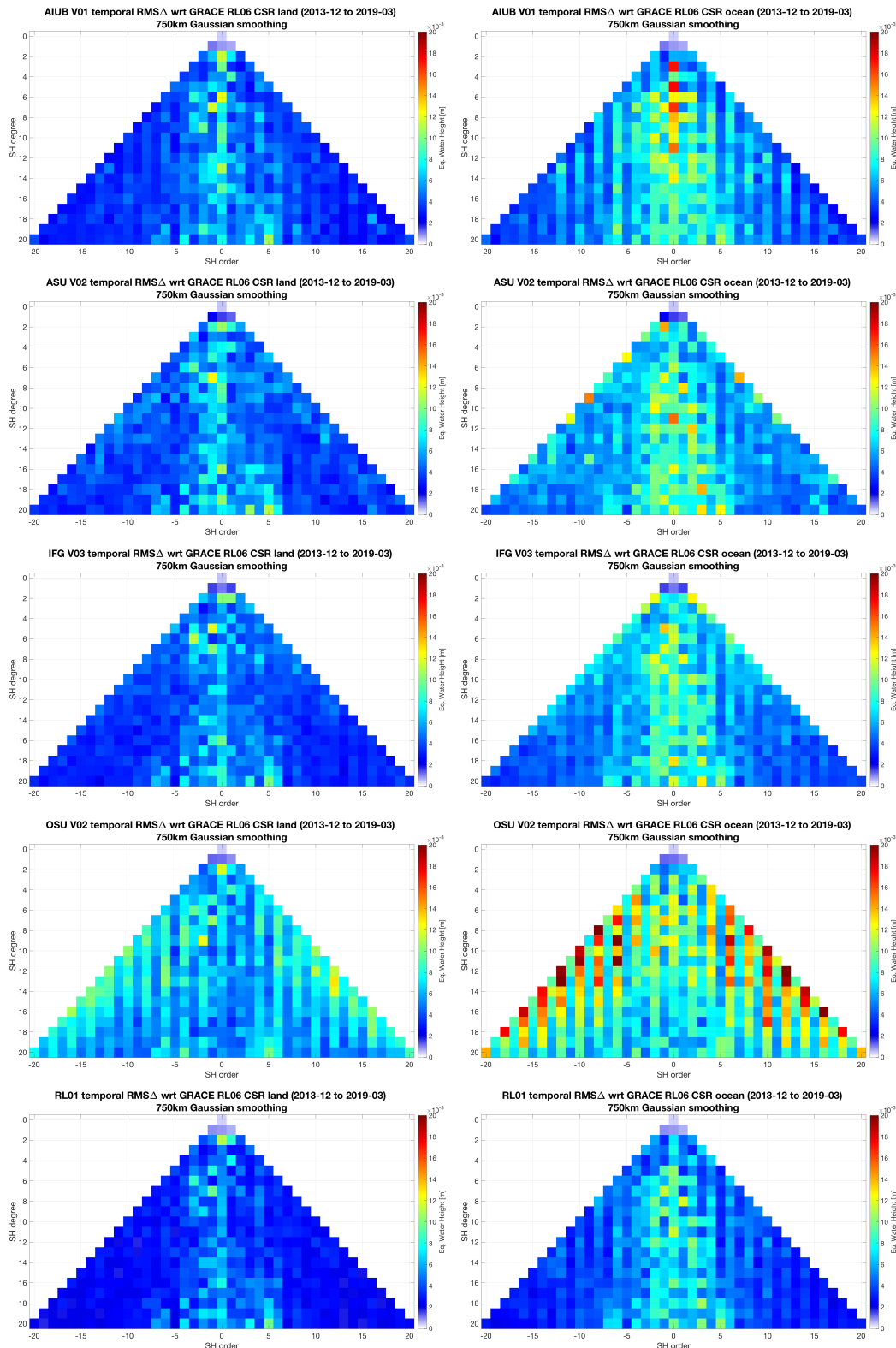


**Figure 9 – Per-coefficient RMS difference between Swarm GFMs and GRACE-based prediction considering 750km Gaussian smoothing, over land (left column) and ocean (right column) areas, for AIUB, ASU, IfG, OSU and combined solutions (respectively from top to bottom).**

### 5.3 Time series of storage catchments

#### 5.3.1 Amazon basin

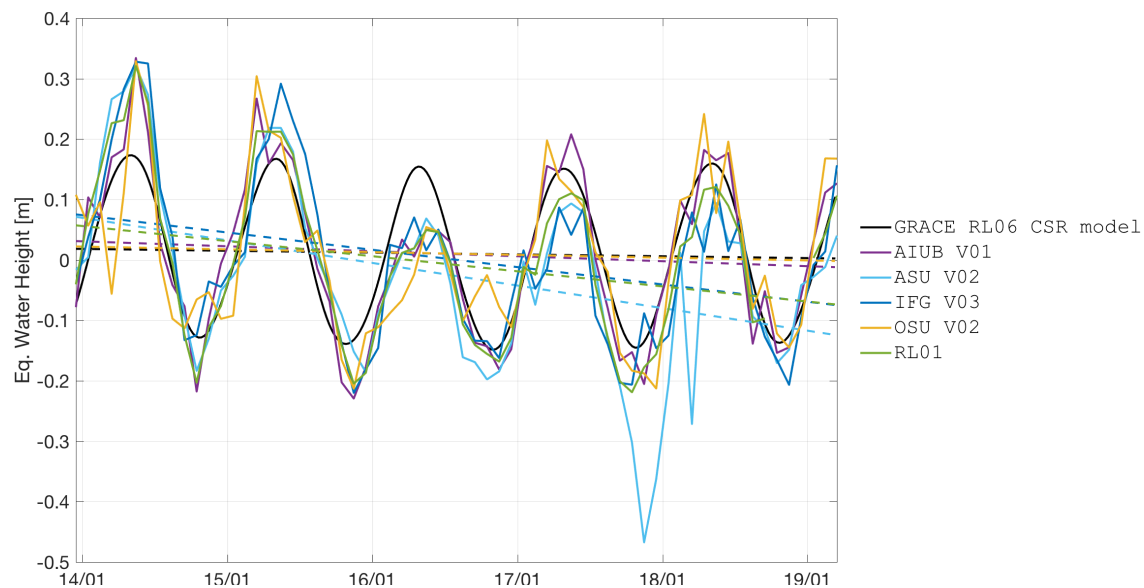


**Figure 10** – Time series of EWH for the Amazon basin (latitude -17 to 3 degrees, longitude -76 to -47 degrees).

solution	constant term [cm]	constant term $\Delta$ [cm]	linear term [cm/year]	linear term $\Delta$ [cm/year]	corr. coeff. []
GRACE RL06 CSR MODEL	2.0	0.0	-0.3	0.0	1.00
AIUB V01	3.6	1.6	-0.8	-0.5	0.92
ASU V02	9.2	7.2	-3.7	-3.4	0.80
IFG V03	9.1	7.1	-2.9	-2.6	0.83
OSU V02	2.5	0.5	-0.5	-0.2	0.82
RL01	7.1	5.1	-2.5	-2.2	0.89

**Table 4** – Statistics of the agreement between the GRACE and Swarm time series for the Amazon basin.

### 5.3.2 Orinoco basin

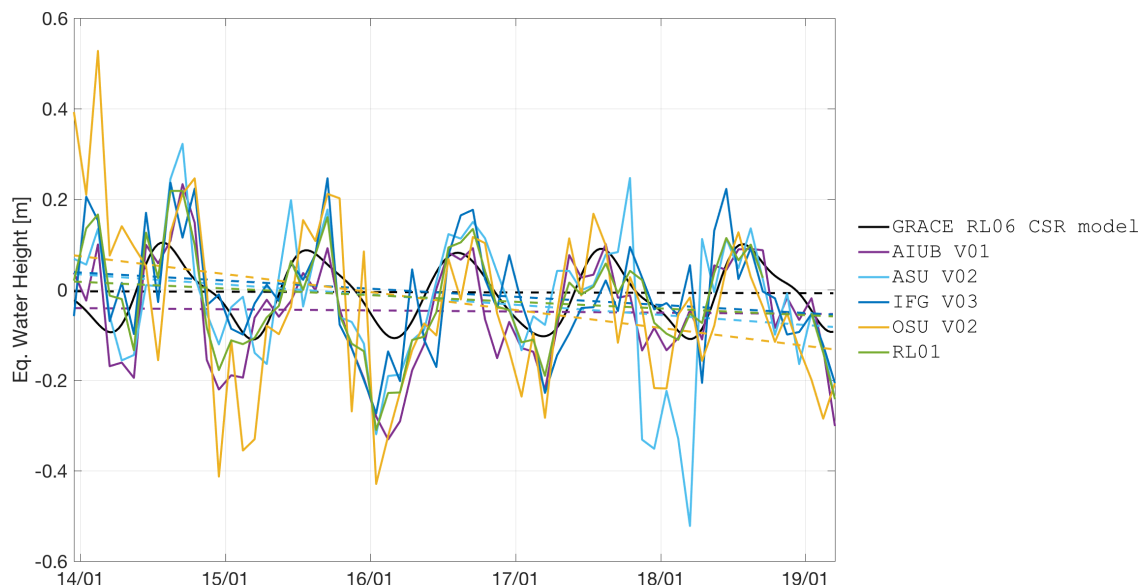


**Figure 11** – Time series of EWH for the Orinoco basin (latitude -3 to 12 degrees, longitude -72 to -59 degrees).

solution	constant term [cm]	constant term $\Delta$ [cm]	linear term [cm/year]	linear term $\Delta$ [cm/year]	corr. coeff. [ ]
GRACE RL06 CSR MODEL	-0.3	0.0	-0.1	0.0	1.00
AIUB V01	-3.9	-3.6	-0.3	-0.2	0.73
ASU V02	4.7	5.0	-2.2	-2.2	0.65
IFG V03	4.8	5.2	-1.8	-1.7	0.55
OSU V02	9.7	10.0	-4.0	-3.9	0.47
RL01	2.6	2.9	-1.5	-1.4	0.70

**Table 5** – Statistics of the agreement between the GRACE and Swarm time series for the Orinoco basin.

### 5.3.3 La Plata basin

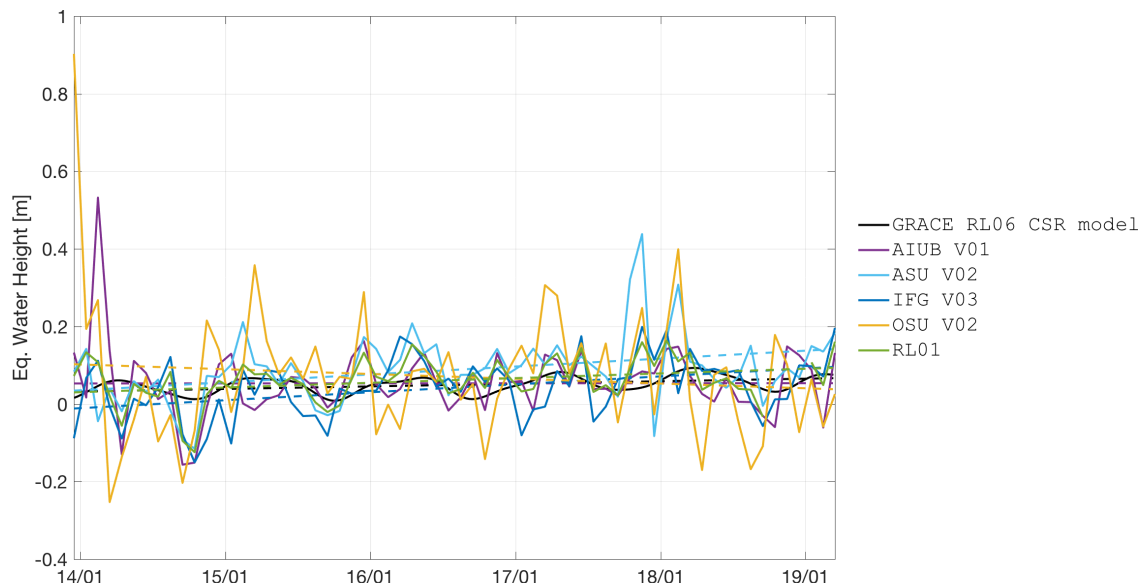


**Figure 12** – Time series of EWH for the La Plata basin (latitude -34 to -19 degrees, longitude -65 to -50 degrees).

solution	constant term [cm]	constant term $\Delta$ [cm]	linear term [cm/year]	linear term $\Delta$ [cm/year]	corr. coeff. [ ]
GRACE RL06 CSR MODEL	2.8	0.0	0.7	0.0	1.00
AIUB V01	5.3	2.5	0.0	-0.7	0.22
ASU V02	2.4	-0.5	2.0	1.4	0.42
IFG V03	-2.3	-5.1	2.0	1.4	0.45
OSU V02	10.9	8.1	-1.2	-1.9	0.05
RL01	2.4	-0.5	1.2	0.5	0.49

**Table 6** – Statistics of the agreement between the GRACE and Swarm time series for the La Plata basin.

### 5.3.4 Mississippi basin

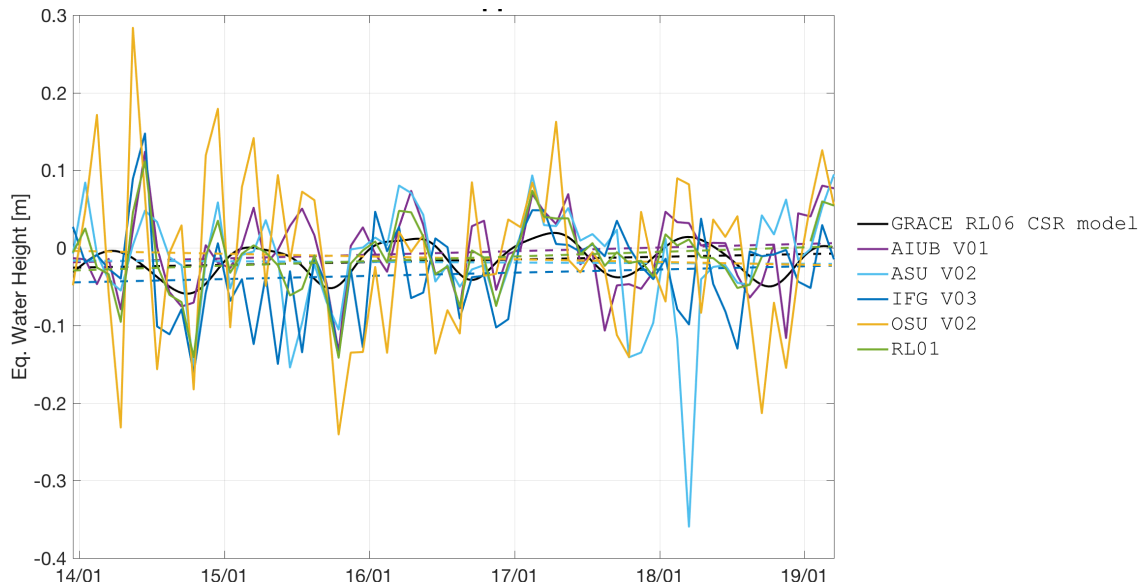


**Figure 13** – Time series of EWH for the Mississippi basin (latitude 29 to 44 degrees, longitude -101 to -80 degrees).

solution	constant term [cm]	constant term $\Delta$ [cm]	linear term [cm/year]	linear term $\Delta$ [cm/year]	corr. coeff. [ ]
GRACE RL06 CSR MODEL	-2.7	0.0	0.3	0.0	1.00
AIUB V01	-2.1	0.6	0.5	0.1	0.58
ASU V02	-1.6	1.1	-0.1	-0.4	0.15
IFG V03	-4.7	-1.9	0.4	0.1	0.27
OSU V02	-0.2	2.5	-0.4	-0.7	0.37
RL01	-3.2	-0.5	0.6	0.2	0.56

**Table 7** – Statistics of the agreement between the GRACE and Swarm time series for the Mississippi basin.

### 5.3.5 Columbia region

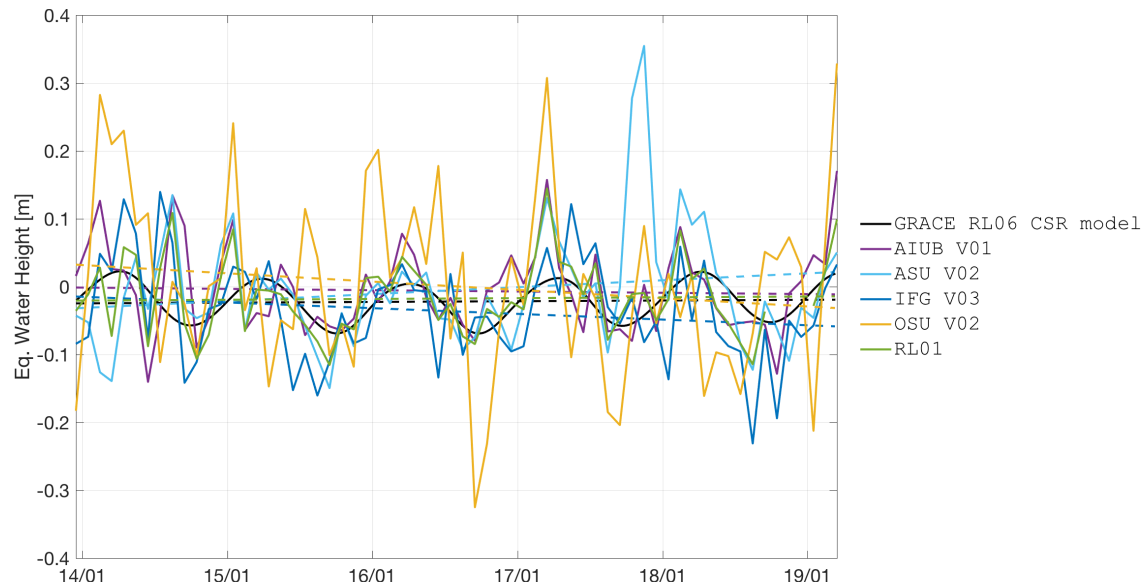


**Figure 14** – Time series of EWH for the Columbia region (latitude 38 to 50 degrees, longitude -125 to -110 degrees).

solution	constant term [cm]	constant term $\Delta$ [cm]	linear term [cm/year]	linear term $\Delta$ [cm/year]	corr. coeff. [ ]
GRACE RL06 CSR MODEL	-2.5	0.0	0.1	0.0	1.00
AIUB V01	-0.0	2.5	-0.2	-0.3	0.45
ASU V02	-3.7	-1.2	1.0	0.9	0.22
IFG V03	-1.0	1.5	-0.8	-0.9	0.54
OSU V02	3.9	6.4	-1.2	-1.3	0.41
RL01	-2.1	0.4	0.1	0.0	0.59

**Table 8** – Statistics of the agreement between the GRACE and Swarm time series for the Columbia region.

### 5.3.6 Alaska

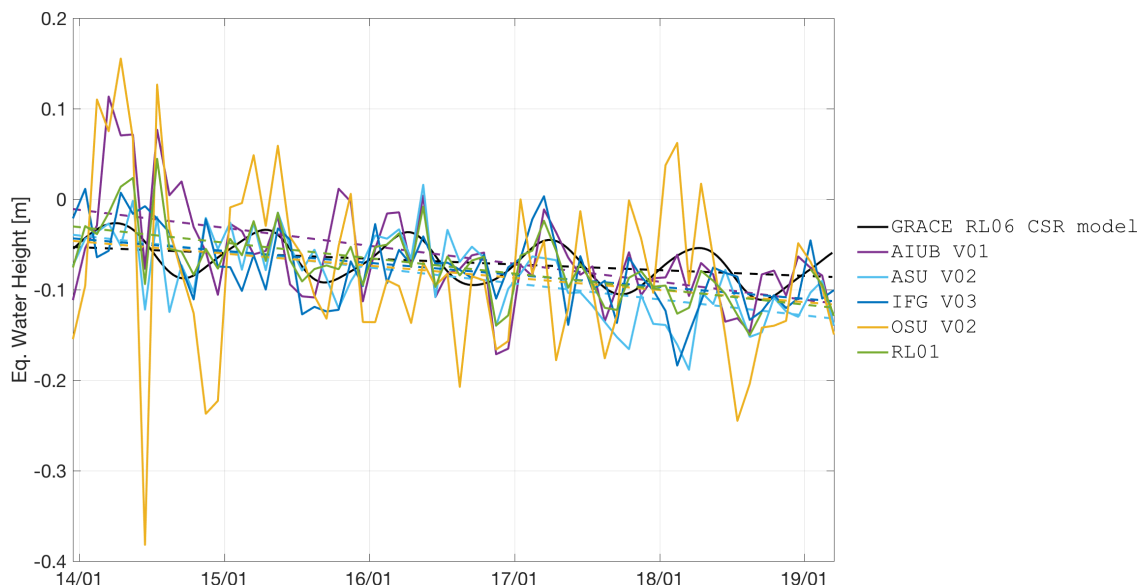


**Figure 15** – Time series of EWH for the Alaska (latitude 56 to 65 degrees, longitude -151 to -129 degrees).

solution	constant term [cm]	constant term $\Delta$ [cm]	linear term [cm/year]	linear term $\Delta$ [cm/year]	corr. coeff. []
GRACE RL06 CSR MODEL	-4.9	0.0	-0.6	0.0	1.00
AIUB V01	-0.0	4.9	-2.0	-1.4	0.50
ASU V02	-3.0	2.0	-1.8	-1.1	0.61
IFG V03	-3.6	1.3	-1.3	-0.7	0.52
OSU V02	-3.9	1.1	-1.3	-0.7	0.46
RL01	-2.1	2.9	-1.7	-1.1	0.67

**Table 9** – Statistics of the agreement between the GRACE and Swarm time series for the Alaska.

### 5.3.7 Western Greenland region

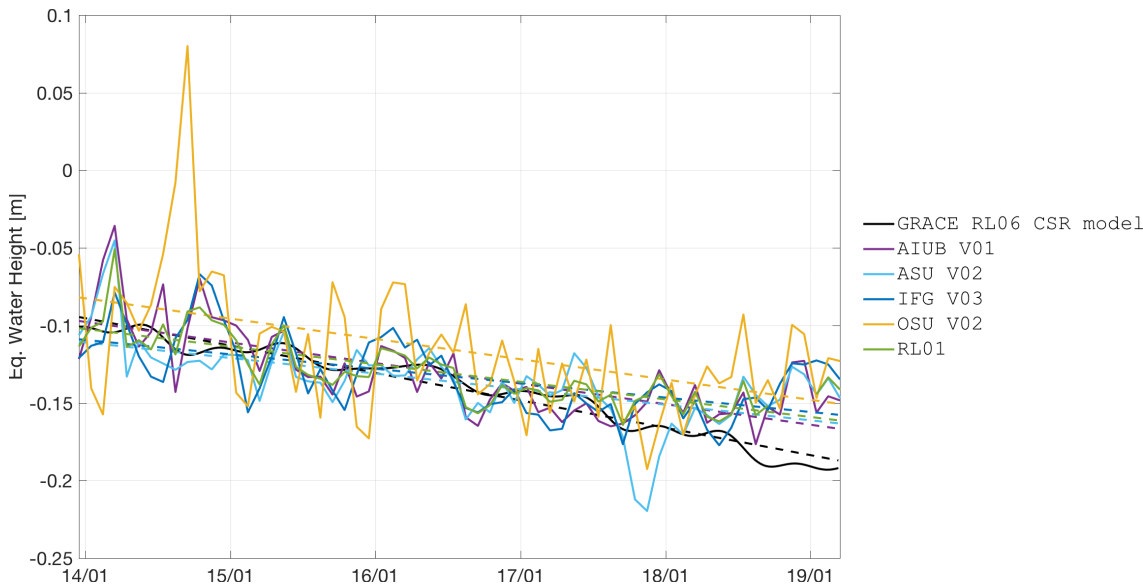


**Figure 16** – Time series of EWH for the Western Greenland region (latitude 60 to 85 degrees, longitude -60 to -37 degrees).

solution	constant term [cm]	constant term $\Delta$ [cm]	linear term [cm/year]	linear term $\Delta$ [cm/year]	corr. coeff. [ ]
GRACE RL06 CSR MODEL	-8.5	0.0	-1.8	0.0	1.00
AIUB V01	-9.0	-0.5	-1.3	0.4	0.71
ASU V02	-10.5	-2.0	-1.0	0.8	0.62
IFG V03	-10.4	-1.9	-0.9	0.8	0.55
OSU V02	-7.5	1.0	-1.3	0.5	0.44
RL01	-9.6	-1.1	-1.1	0.6	0.77

**Table 10** – Statistics of the agreement between the GRACE and Swarm time series for the Western Greenland region.

### 5.3.8 Danube basin

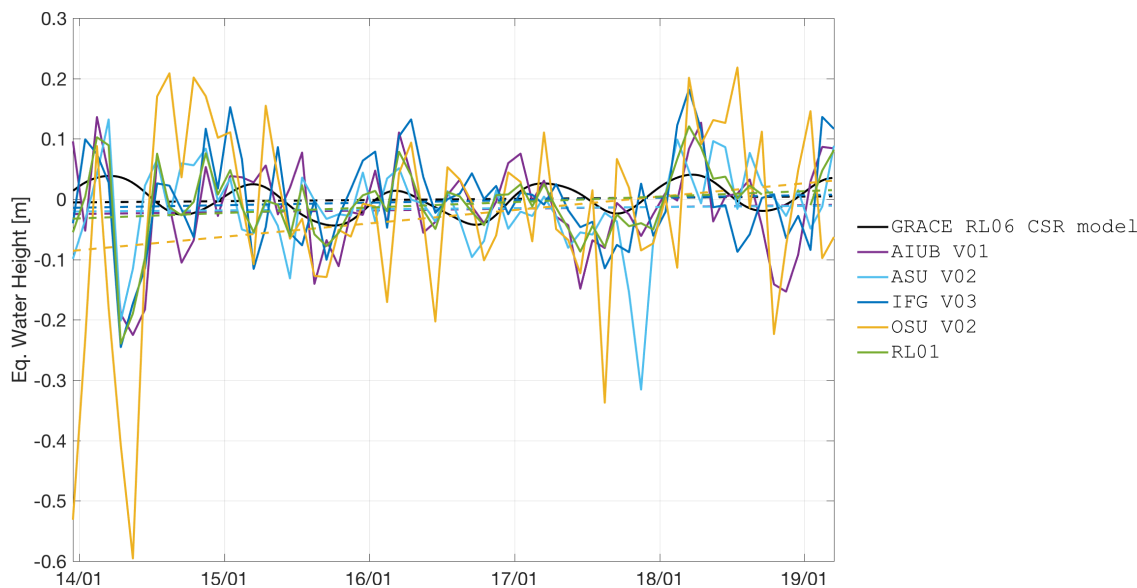


**Figure 17** – Time series of EWH for the Danube basin (latitude 43 to 48 degrees, longitude 13 to 28 degrees).

solution	constant term [cm]	constant term $\Delta$ [cm]	linear term [cm/year]	linear term $\Delta$ [cm/year]	corr. coeff. [ ]
GRACE RL06 CSR MODEL	-0.6	0.0	0.2	0.0	1.00
AIUB V01	-2.6	-2.0	0.3	0.1	0.27
ASU V02	-2.1	-1.5	0.2	-0.0	0.11
IFG V03	-1.7	-1.0	0.4	0.2	0.20
OSU V02	-9.7	-9.1	2.2	2.0	-0.10
RL01	-3.7	-3.1	0.9	0.7	0.22

**Table 11** – Statistics of the agreement between the GRACE and Swarm time series for the Danube basin.

### 5.3.9 Western Sub-Saharan basin

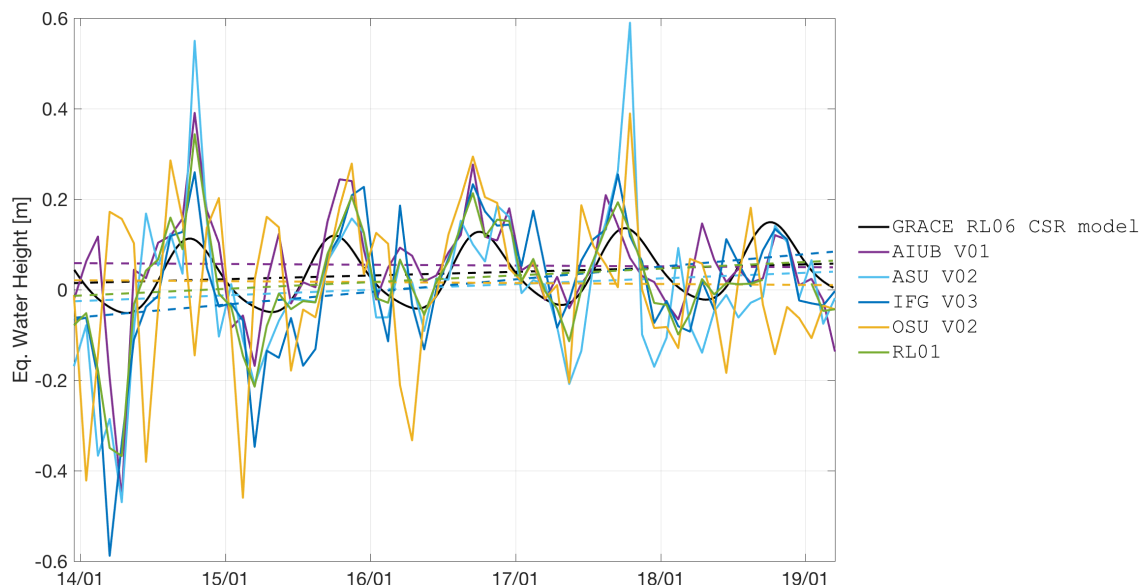


**Figure 18** – Time series of EWH for the Western Sub-Saharan basin (latitude 5 to 15 degrees, longitude -15 to -1 degrees).

solution	constant term [cm]	constant term $\Delta$ [cm]	linear term [cm/year]	linear term $\Delta$ [cm/year]	corr. coeff. [ ]
GRACE RL06 CSR MODEL	1.0	0.0	0.8	0.0	1.00
AIUB V01	6.0	4.9	-0.2	-1.0	0.59
ASU V02	-3.2	-4.3	1.2	0.4	0.65
IFG V03	-7.7	-8.7	2.8	2.0	0.67
OSU V02	2.2	1.2	-0.2	-1.0	0.38
RL01	-2.2	-3.2	1.5	0.7	0.68

**Table 12** – Statistics of the agreement between the GRACE and Swarm time series for the Western Sub-Saharan basin.

### 5.3.10 Eastern Sub-Saharan basin

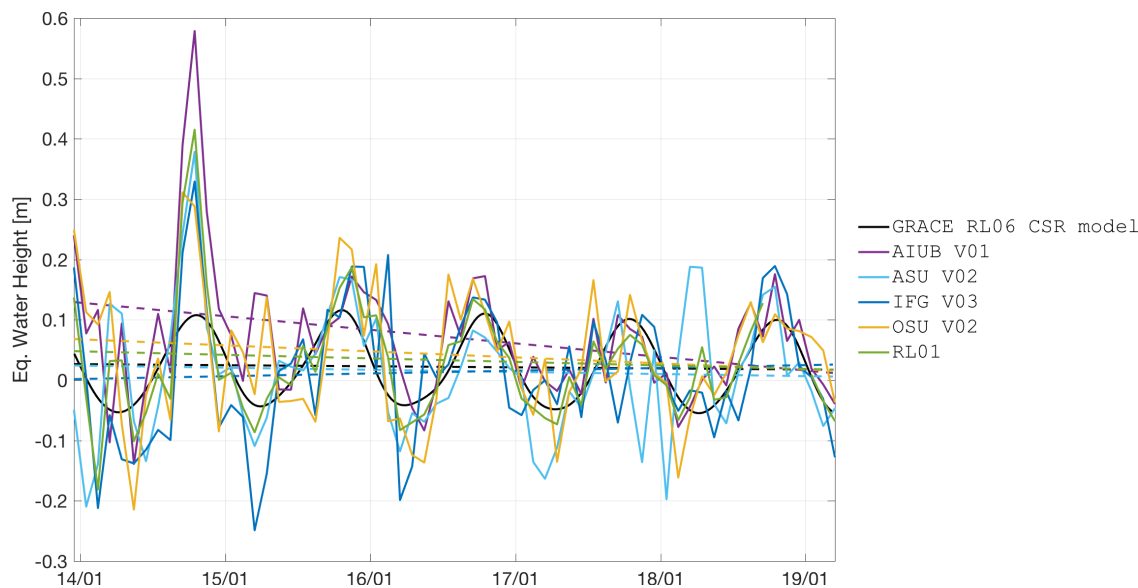


**Figure 19** – Time series of EWH for the Eastern Sub-Saharan basin (latitude 1 to 13 degrees, longitude -8 to 35 degrees).

solution	constant term [cm]	constant term $\Delta$ [cm]	linear term [cm/year]	linear term $\Delta$ [cm/year]	corr. coeff. [ ]
GRACE RL06 CSR MODEL	2.8	0.0	-0.2	0.0	1.00
AIUB V01	14.2	11.4	-2.2	-2.1	0.63
ASU V02	2.6	-0.1	-0.4	-0.2	0.54
IFG V03	-0.1	-2.8	0.5	0.6	0.71
OSU V02	7.4	4.6	-1.0	-0.8	0.62
RL01	5.1	2.4	-0.6	-0.4	0.77

**Table 13** – Statistics of the agreement between the GRACE and Swarm time series for the Eastern Sub-Saharan basin.

### 5.3.11 Congo and Zambezi basins

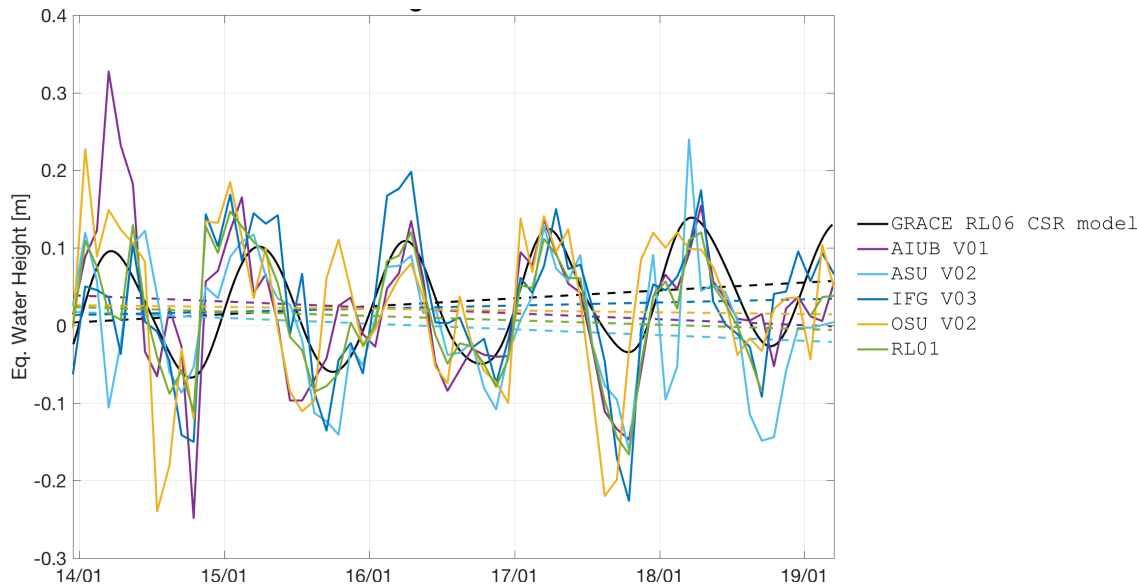


**Figure 20** – Time series of EWH for the Congo and Zambezi basins (latitude -23 to -3 degrees, longitude 14 to 38 degrees).

solution	constant term [cm]	constant term $\Delta$ [cm]	linear term [cm/year]	linear term $\Delta$ [cm/year]	corr. coeff. [ ]
GRACE RL06 CSR MODEL	-0.2	0.0	1.0	0.0	1.00
AIUB V01	4.3	4.5	-0.8	-1.8	0.67
ASU V02	2.1	2.3	-0.7	-1.8	0.67
IFG V03	1.1	1.3	0.4	-0.6	0.73
OSU V02	2.7	2.9	-0.2	-1.3	0.52
RL01	2.7	2.9	-0.6	-1.6	0.75

**Table 14** – Statistics of the agreement between the GRACE and Swarm time series for the Congo and Zambezi basins.

### 5.3.12 Volga basin

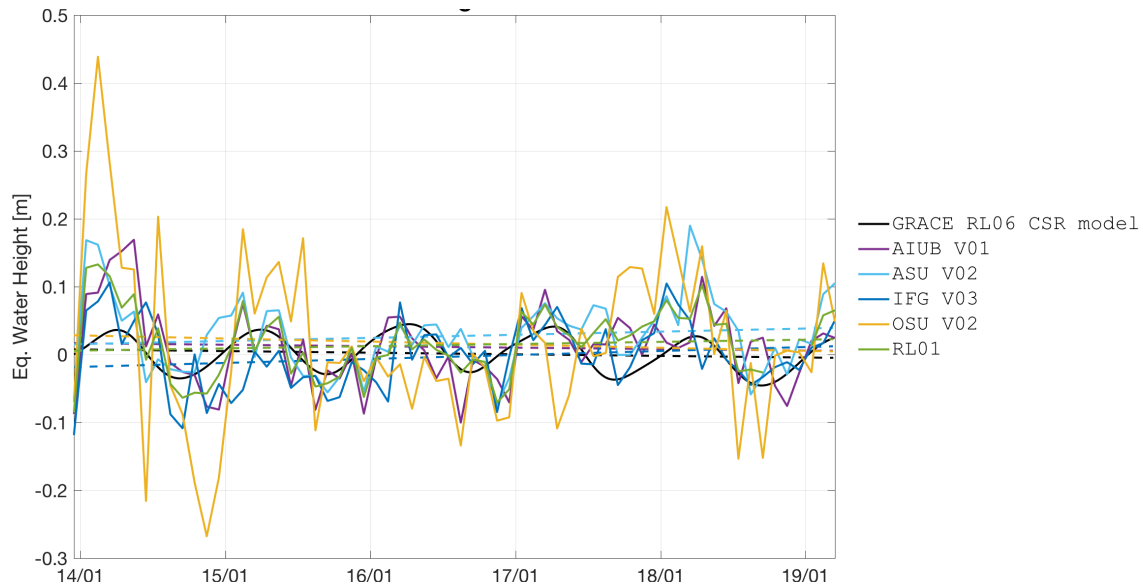


**Figure 21** – Time series of EWH for the Volga basin (latitude 53 to 61 degrees, longitude 34 to 56 degrees).

solution	constant term [cm]	constant term $\Delta$ [cm]	linear term [cm/year]	linear term $\Delta$ [cm/year]	corr. coeff. [ ]
GRACE RL06 CSR MODEL	0.9	0.0	-0.2	0.0	1.00
AIUB V01	1.8	0.9	-0.2	0.0	0.50
ASU V02	1.3	0.4	0.5	0.7	0.53
IFG V03	-2.2	-3.0	0.6	0.8	0.48
OSU V02	3.1	2.2	-0.5	-0.2	0.32
RL01	0.4	-0.5	0.3	0.6	0.55

**Table 15** – Statistics of the agreement between the GRACE and Swarm time series for the Volga basin.

### 5.3.13 Siberia region

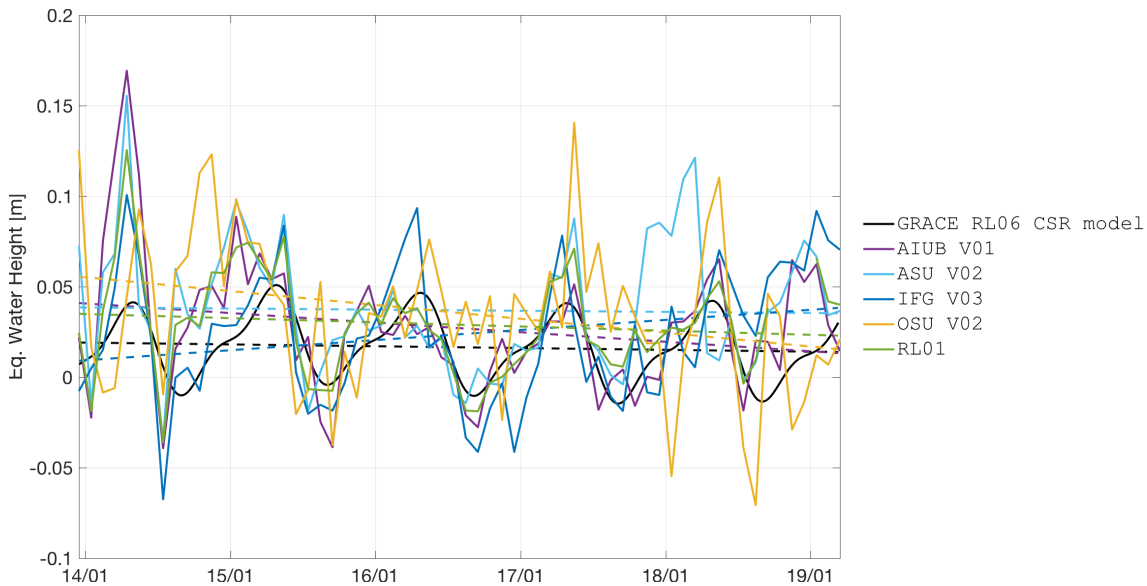


**Figure 22** – Time series of EWH for the Siberia region (latitude 57 to 72 degrees, longitude 68 to 109 degrees).

solution	constant term [cm]	constant term $\Delta$ [cm]	linear term [cm/year]	linear term $\Delta$ [cm/year]	corr. coeff. [ ]
GRACE RL06 CSR MODEL	2.0	0.0	-0.1	0.0	1.00
AIUB V01	4.4	2.4	-0.5	-0.4	0.58
ASU V02	3.9	1.9	-0.1	0.0	0.42
IFG V03	0.6	-1.4	0.6	0.7	0.60
OSU V02	6.0	4.0	-0.8	-0.7	0.31
RL01	3.6	1.7	-0.2	-0.1	0.62

**Table 16** – Statistics of the agreement between the GRACE and Swarm time series for the Siberia region.

### 5.3.14 Ganges-Brahmaputra basin

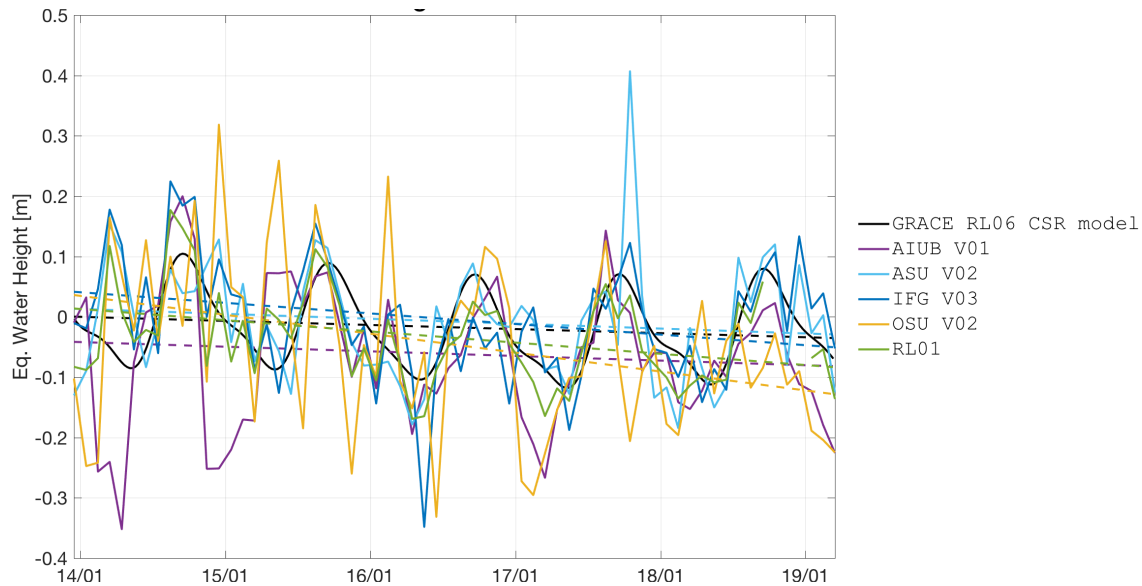


**Figure 23** – Time series of EWH for the Ganges-Brahmaputra basin (latitude 15 to 30 degrees, longitude 72 to 89 degrees).

solution	constant term [cm]	constant term $\Delta$ [cm]	linear term [cm/year]	linear term $\Delta$ [cm/year]	corr. coeff. [ ]
GRACE RL06 CSR MODEL	0.4	0.0	-0.7	0.0	1.00
AIUB V01	-3.7	-4.1	-0.8	-0.1	0.56
ASU V02	1.8	1.4	-0.8	-0.1	0.63
IFG V03	5.1	4.7	-1.8	-1.1	0.65
OSU V02	5.3	4.9	-3.1	-2.5	0.27
RL01	2.4	2.0	-1.9	-1.2	0.75

**Table 17** – Statistics of the agreement between the GRACE and Swarm time series for the Ganges-Brahmaputra basin.

### 5.3.15 Indochina region

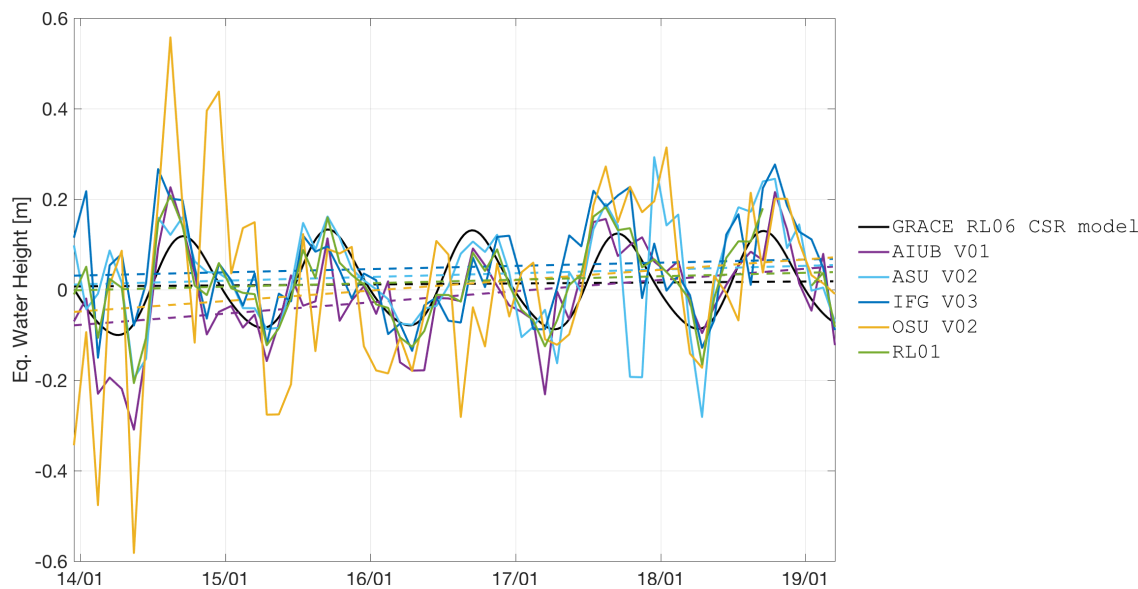


**Figure 24** – Time series of EWH for the Indochina region (latitude 12 to 29 degrees, longitude 93 to 105 degrees).

solution	constant term [cm]	constant term $\Delta$ [cm]	linear term [cm/year]	linear term $\Delta$ [cm/year]	corr. coeff. [ ]
GRACE RL06 CSR MODEL	0.6	0.0	0.2	0.0	1.00
AIUB V01	-9.2	-9.8	2.5	2.3	0.72
ASU V02	0.7	0.1	0.8	0.6	0.63
IFG V03	2.7	2.1	0.7	0.5	0.58
OSU V02	-6.2	-6.8	2.3	2.1	0.46
RL01	-0.6	-1.2	0.8	0.6	0.78

**Table 18** – Statistics of the agreement between the GRACE and Swarm time series for the Indochina region.

### 5.3.16 Northern Australia region

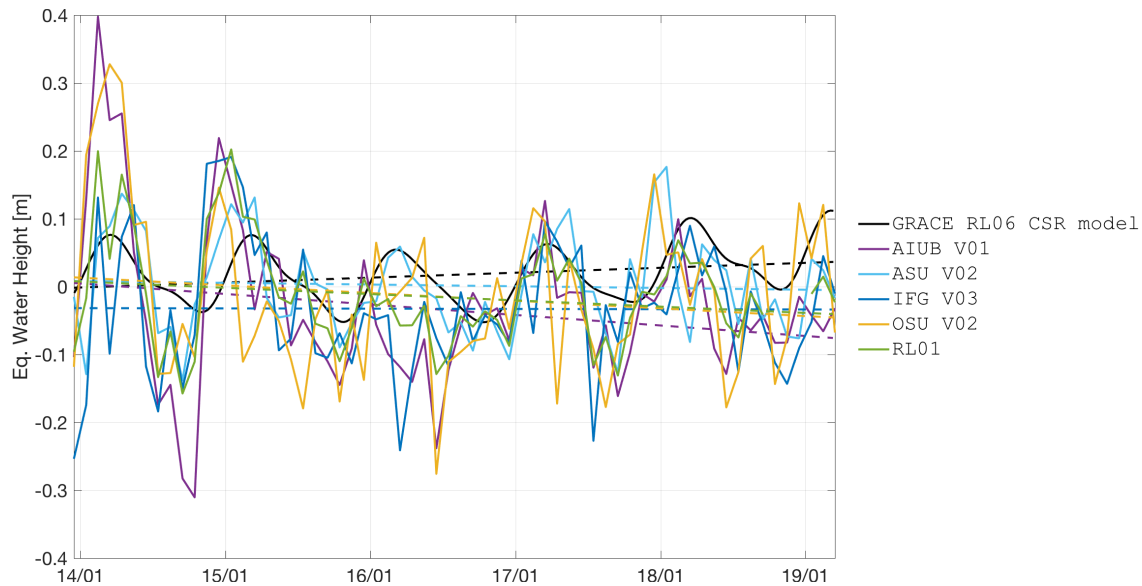


**Figure 25** – Time series of EWH for the Northern Australia region (latitude -24 to -10 degrees, longitude 124 to 145 degrees).

solution	constant term [cm]	constant term $\Delta$ [cm]	linear term [cm/year]	linear term $\Delta$ [cm/year]	corr. coeff. [ ]
GRACE RL06 CSR MODEL	-0.5	0.0	0.7	0.0	1.00
AIUB V01	1.4	1.9	-1.5	-2.3	0.41
ASU V02	1.0	1.5	-0.3	-1.0	0.52
IFG V03	-3.1	-2.6	-0.0	-0.8	0.35
OSU V02	2.0	2.5	-1.1	-1.9	0.42
RL01	1.3	1.8	-0.9	-1.7	0.53

**Table 19** – Statistics of the agreement between the GRACE and Swarm time series for the Northern Australia region.

### 5.3.17 Western Antarctica region

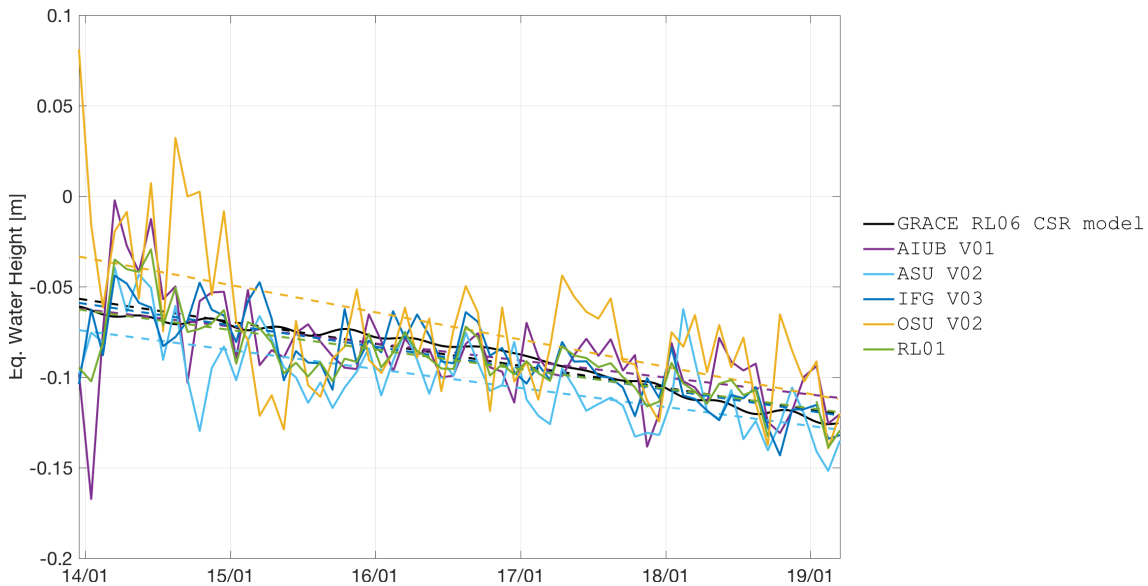


**Figure 26** – Time series of EWH for the Western Antarctica region (latitude -80 to -70 degrees, longitude -140 to -85 degrees).

solution	constant term [cm]	constant term $\Delta$ [cm]	linear term [cm/year]	linear term $\Delta$ [cm/year]	corr. coeff. [ ]
GRACE RL06 CSR MODEL	-5.0	0.0	-1.2	0.0	1.00
AIUB V01	-5.7	-0.7	-0.9	0.3	0.56
ASU V02	-6.8	-1.8	-1.0	0.2	0.70
IFG V03	-5.3	-0.2	-1.2	0.0	0.86
OSU V02	-2.5	2.5	-1.5	-0.3	0.52
RL01	-5.7	-0.7	-1.1	0.1	0.78

**Table 20** – Statistics of the agreement between the GRACE and Swarm time series for the Western Antarctica region.

### 5.3.18 Eastern Antarctica region

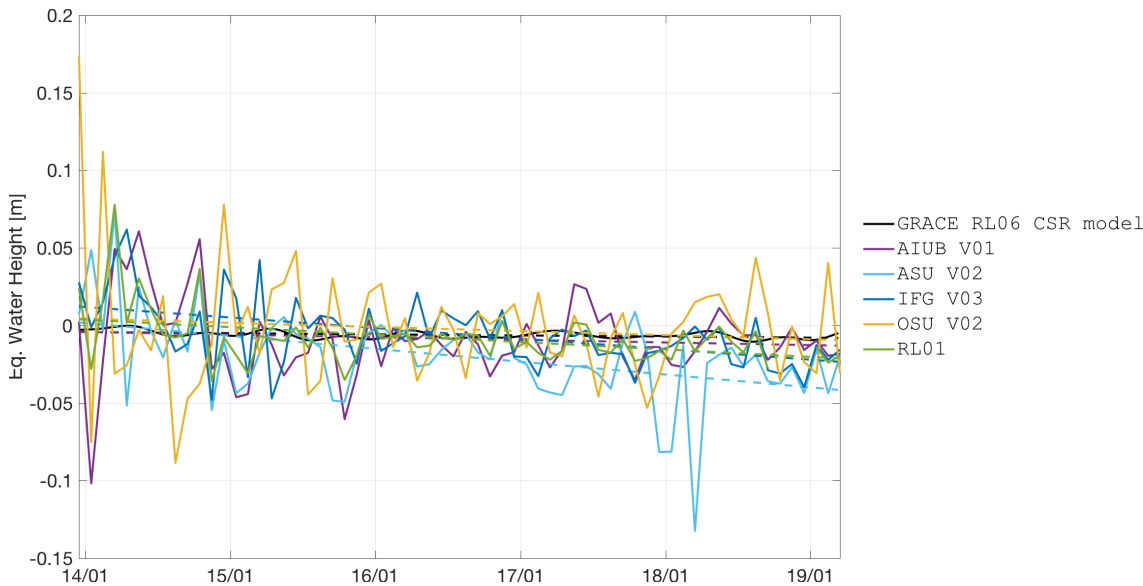


**Figure 27** – Time series of EWH for the Eastern Antarctica region (latitude -80 to -68 degrees, longitude 80 to 130 degrees).

solution	constant term [cm]	constant term $\Delta$ [cm]	linear term [cm/year]	linear term $\Delta$ [cm/year]	corr. coeff. [ ]
GRACE RL06 CSR MODEL	-0.4	0.0	-0.1	0.0	1.00
AIUB V01	-0.3	0.1	-0.2	-0.1	0.27
ASU V02	0.6	1.0	-0.8	-0.8	0.23
IFG V03	1.6	2.0	-0.7	-0.6	0.44
OSU V02	0.6	1.0	-0.3	-0.2	0.11
RL01	0.7	1.0	-0.5	-0.4	0.48

**Table 21** – Statistics of the agreement between the GRACE and Swarm time series for the Eastern Antarctica region.

### 5.3.19 Overview

solution	constant term $\Delta$ RMS [cm]	linear term $\Delta$ RMS [cm/year]	corr. coeff. mean [ ]
GRACE RL06 CSR model	0.00	0.00	1.00
aiub v01	4.44	1.10	0.55
asu ifg v02	2.64	1.22	0.51
ifg v03	3.72	1.10	0.55
osu aiub v02	4.91	1.55	0.38
sh rl01	2.25	0.98	0.64

**Table 22** – Statistics of the agreement between the GRACE and Swarm time series for the regions displayed in Sections 5.3.1 to 5.3.18.

## 5.4 Temporal variability

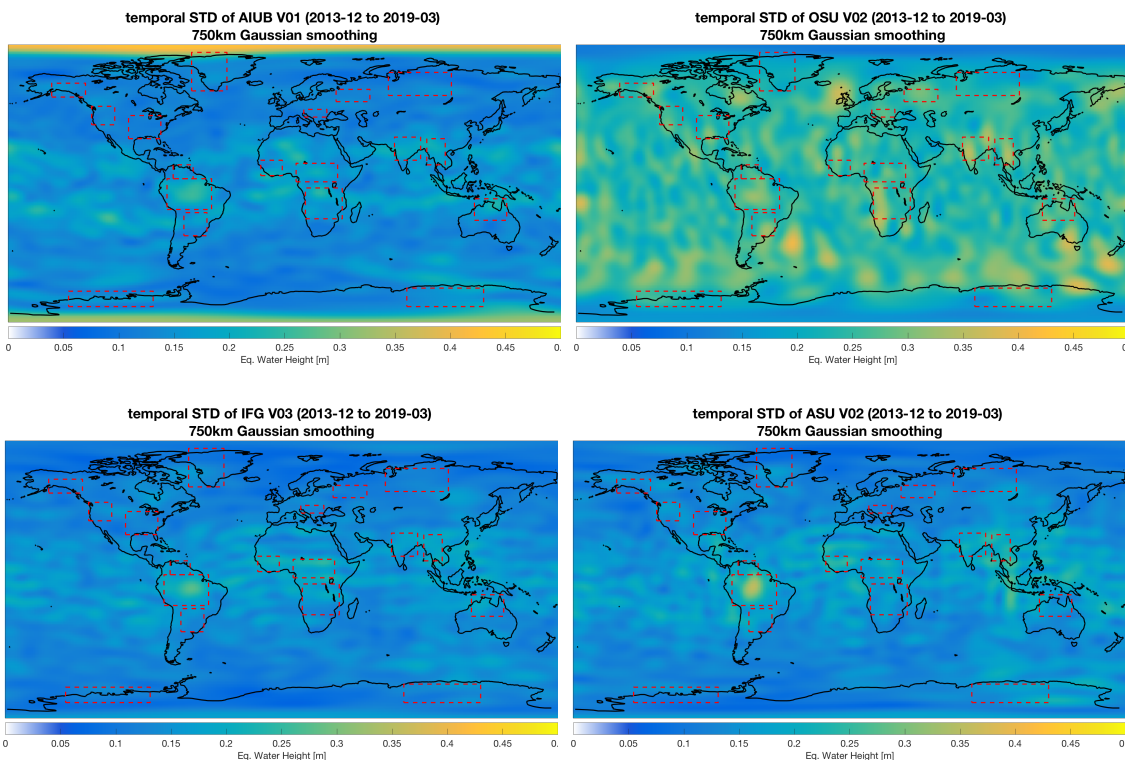


**Figure 28** – Temporal variability of the individual solutions

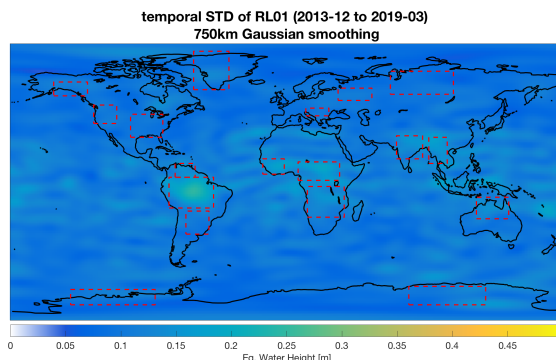


**Figure 29** – Temporal variability of the combined solutions

## Acronyms

<b>AA</b>	Acceleration Approach, Rummel (1979)
<b>AIUB</b>	Astronomical Institute of the University of Bern, Switzerland, <a href="http://www.aiub.unibe.ch">www.aiub.unibe.ch</a>
<b>ASU</b>	Astronomical Institute (Astronomický ústav), AVCR, Ondřejov, <a href="http://www.asu.cas.cz/en">www.asu.cas.cz/en</a>
<b>AVCR</b>	Czech Academy of Sciences (Akademie věd České Republiky), Czech Republic, <a href="http://www.avcr.cz/en/">www.avcr.cz/en/</a>
<b>CSR</b>	Center for Space Research, UTexas, USA, <a href="http://www.cs.utexas.edu">www.cs.utexas.edu</a>
<b>EBA</b>	Energy Balance Approach, O'Keefe (1957) and Jekeli (1999)
<b>EW</b>	Equivalent Water Height
<b>GFM</b>	Gravity Field Model
<b>GRACE</b>	Gravity Recovery And Climate Experiment, Tapley, Reigber and Melbourne (1996) and Tapley (2004)
<b>IfG</b>	Institute of Geodesy, TUG, Graz, <a href="http://www.ifg.tugraz.at">www.ifg.tugraz.at</a>
<b>KO</b>	Kinematic Orbit
<b>N/A</b>	Not Applicable
<b>NEQ</b>	Normal Equation
<b>OSU</b>	Ohio State University, <a href="http://www.osu.edu">www.osu.edu</a>
<b>RL06</b>	Release 6
<b>RMS</b>	Root Mean Squared
<b>SH</b>	Spherical Harmonic
<b>SLR</b>	Satellite Laser Ranging, Smith and Turcotte (1993) and Combrinck (2010)
<b>TU Delft</b>	Delft University of Technology, Netherlands, <a href="http://www.tudelft.nl">www.tudelft.nl</a>
<b>TUG</b>	Graz University of Technology, Austria, <a href="http://www.tugraz.at">www.tugraz.at</a>
<b>UTexas</b>	University of Texas at Austin, <a href="http://www.utexas.edu">www.utexas.edu</a>
<b>USA</b>	United States of America
<b>VCE</b>	Variance Component Estimation
<b>WP</b>	Work Package

## References

- Beutler, Gerhard et al. (2010). **The celestial mechanics approach: theoretical foundations.** In: *J. Geod.* 84.10, pp. 605–624. DOI: 10.1007/s00190-010-0401-7 (cit. on p. 7).
- Bezděk, Aleš et al. (2014). **Gravity field models from kinematic orbits of CHAMP, GRACE and GOCE satellites.** In: *Adv. Sp. Res.* 53.3, pp. 412–429. DOI: 10.1016/j.asr.2013.11.031 (cit. on p. 7).
- Bezděk, Aleš et al. (2016). **Time-variable gravity fields derived from GPS tracking of Swarm.** In: *Geophys. J. Int.* 205.3, pp. 1665–1669. DOI: 10.1093/gji/ggw094 (cit. on p. 7).
- Cheng, M. and John Ries (2018). **GRACE Technical Note 11: Monthly estimates of C20 from 5 satellites based on GRACE RL06 models.** Austin, USA. URL: [ftp://podaac-ftp.jpl.nasa.gov/allData/grace/docs/TN-11\\_C20\\_SLR.txt](ftp://podaac-ftp.jpl.nasa.gov/allData/grace/docs/TN-11_C20_SLR.txt) (cit. on pp. 8, 9).
- Combrinck, Ludwig (2010). **Satellite Laser Ranging.** In: *Sci. Geod. - I.* Ed. by Guochang Xu. Berlin, Heidelberg: Springer Berlin Heidelberg. Chap. 9, pp. 301–338. DOI: 10.1007/978-3-642-11741-1\_9 (cit. on p. 36).
- de Teixeira da Encarnação, João and Pieter Visser (2019). **TN-03: Swarm models validation.** Tech. rep. TU Delft. URL: [https://jgte.github.io/gswarm/Documents/SW\\_TN\\_DUT\\_GS\\_0003\\_TN-03\\_Validation.1.1.1.pdf](https://jgte.github.io/gswarm/Documents/SW_TN_DUT_GS_0003_TN-03_Validation.1.1.1.pdf) (cit. on pp. 7, 8).
- Guo, J. Y., X. J. Duan and C. K. Shum (2010). **Non-isotropic Gaussian smoothing and leakage reduction for determining mass changes over land and ocean using GRACE data.** In: *Geophys. J. Int.* 181.1, pp. 290–302. DOI: 10.1111/j.1365-246X.2010.04534.x (cit. on p. 10).
- Guo, J. Y. et al. (2015). **On the energy integral formulation of gravitational potential differences from satellite-to-satellite tracking.** In: *Celest. Mech. Dyn. Astron.* 121.4, pp. 415–429. DOI: 10.1007/s10569-015-9610-y (cit. on p. 7).
- Jäggi, A. et al. (2016). **Swarm kinematic orbits and gravity fields from 18 months of GPS data.** In: *Adv. Sp. Res.* 57.1, pp. 218–233. DOI: 10.1016/j.asr.2015.10.035 (cit. on p. 7).
- Jekeli, Christopher (1999). **The determination of gravitational potential differences from satellite-to-satellite tracking.** In: *Celest. Mech. Dyn. Astron.* 75.2, pp. 85–101. DOI: 10.1023/A:1008313405488 (cit. on p. 36).
- Mayer-Gürr, Torsten (2006). **Gravitationsfeldbestimmung aus der Analyse kurzer Bahnbögen am Beispiel der Satellitenmissionen CHAMP und GRACE.** PhD thesis. Rheinischen Friedrich-Wilhelms Universität Bonn. URL: <http://hss.ulb.uni-bonn.de/2006/0904/0904.pdf> (cit. on p. 7).
- O'Keefe, John A. (1957). **An application of Jacobi's integral to the motion of an earth satellite.** In: *Astron. J.* 62, p. 265. DOI: 10.1086/107530 (cit. on p. 36).
- Rummel, R. (1979). **Determination of short-wavelength components of the gravity field from satellite-to-satellite tracking or satellite gradiometry.** In: *Manuscripta Geod.* 4.2, pp. 107–148 (cit. on p. 36).
- Shang, Kun et al. (2015). **GRACE time-variable gravity field recovery using an improved energy balance approach.** In: *Geophys. J. Int.* 203.3, pp. 1773–1786. DOI: 10.1093/gji/ggv392 (cit. on p. 7).
- Smith, David E. and Donald L. Turcotte (1993). **Millimeter Accuracy Satellite Laser Ranging: a Review.** In: *Contrib. Sp. Geod. to Geodyn. Technol.* Ed. by John J. Degnan. Vol. 25. Geodynamics Series. Washington, D. C.: American Geophysical Union. DOI: 10.1029/GD025p0133 (cit. on p. 36).
- Tapley, B., C. Reigber and W Melbourne (1996). **Gravity Recovery And Climate Experiment (GRACE) mission.** Baltimore, USA (cit. on p. 36).

- Tapley, B.~D. et al. (2013). **The Status and Future Prospect for GRACE After the First Decade.** In: *AGU Fall Meet. Abstract G32A-01*. San Francisco, CA, USA. URL: <http://abstractsearch.agu.org/meetings/2013/FM/G32A-01.html> (cit. on p. 9).
- Tapley, Byron D. (2004). **GRACE Measurements of Mass Variability in the Earth System.** In: *Science* (80-). 305.5683, pp. 503–505. DOI: 10.1126/science.1099192 (cit. on p. 36).
- Teixeira Encarnaçāo, Joao and Pieter Visser (2017). **TN-01 : Standards and Background Models.** Tech. rep. Delft, the Netherlands: Delft University of Technology. URL: <http://jgte.github.io/gswarm/TN-01/TN-01.pdf> (cit. on p. 7).
- Zehentner, Norbert and Torsten Mayer-Gürr (2016). **Precise orbit determination based on raw GPS measurements.** In: *J. Geod.* 90.3, pp. 275–286. DOI: 10.1007/s00190-015-0872-7 (cit. on p. 7).